

ISLAM ARIDA

**MECHANICAL ADAPTABILITY FOR
LIGHT-RESPONSIVE LIQUID CRYSTAL
NETWORKS VIA INCORPORATING
ACRYLIC ACID**

Master's Thesis

Faculty of Medicine and Health
Technology
M.Sc. (Tech.)
April 2023

ABSTRACT

Islam Arida: Mechanical Adaptability for Light-Responsive Liquid Crystal Networks via Incorporating Acrylic Acid
Master's Thesis in Technology
Tampere University
Biomedical Sciences and Engineering – Biomaterials and Tissue Engineering
April 2023

The field of soft robotics has gained huge interest in the field of robotics due to the versatility, compliance and flexibility of soft actuators compared to their rigid counterparts. Liquid crystal networks (LCNs), especially light-responsive LCNs provide a promising platform for designing soft actuators due to their excellent high deformation ability and mechanical properties. Mechanical adaptability, i.e., spontaneous change in mechanical properties in response to changes in the surrounding conditions, of LCN-based soft actuators is a convenient feature to be considered when designing a soft robot. Such feature provides the ability to function in different environmental conditions with different constraints to the mechanical properties of the actuator. Here, liquid crystal (LC) mixtures were prepared with varied molar ratios of acrylic acid. Phase transition points were identified for the LC mixtures. Selected LC mixtures were polymerized to prepare light-responsive LCN films. Characterization of these films as well as investigation of their mechanical adaptability were carried out. The results showed that the mechanical adaptability capacity increased as the monomer-to-acrylic-acid molar ratio (M_{AA}) decreased. However, the downside was that the overall mechanical strength and the nematic alignment of the films were reduced. LCN films with M_{AA} of 1:1 and 1:2 possessed the best balance of efficient mechanical adaptability while maintaining good mechanical strength and nematic alignment. Optimizing the molar ratios of acrylic acid and investigating other techniques of incorporating acrylic acid into the network is an important next step to this work. Furthermore, this work can open the possibility of designing a mechanical adaptable light-responsive soft robot.

Keywords: soft actuators, liquid crystal networks, light-responsive materials, azobenzenes, acrylic acid

The originality of this thesis has been checked using the Turnitin OriginalityCheck service.

PREFACE

This thesis was carried out in the RedLabs laboratories at the Material Science and environmental Engineering unit at Tampere University in 2023.

Firstly, I would like to thank my supervisor Prof. Arri Priimägi for allowing me to join Smart Photonic Materials (SPM) research group as a trainee first and then as a research assistant to conduct my master's thesis. I would like to thank my co-supervisor Zixuan Deng for his continuous support and guidance throughout my work.

I would like to also thank Mari Isomäki and Chiara Fedele for their continuous guidance during my traineeship. In addition, I am grateful to the rest of the members of SPM group for their kind support and the welcoming atmosphere they have created for me.

I would like to thank everyone in the faculty of Medicine and Health Technology for their help with any problem I have faced during my studies and their valuable advice. I am also thankful to all the friends I have made since enrolling in Tampere University for the joyful moments we had together.

Finally, I would like to express my gratitude to my parents, family, and friends in Egypt for believing in me and the support they have provided for me to keep going.

Tampere, 25 April 2023

Islam Arida

CONTENTS

1. INTRODUCTION	1
2. LITERATURE REVIEW.....	3
2.1 Liquid Crystal and Liquid Crystal Materials.....	3
2.2 Thermotropic Liquid Crystal Networks.....	5
2.3 Light Responsivity.....	6
2.4 Mechanical Adaptability	6
3. MATERIALS AND METHODS	8
3.1 Preparation of LC Mixtures.....	8
3.2 Phase Transition Identification	9
3.3 Preparation of LCN Films	10
3.4 Characterization of LCN Films	12
3.4.1 Nematic LC Alignment	12
3.4.2 Order Parameter	12
3.4.3 Thermal Actuation.....	13
3.4.4 Mechanical Properties and Adaptability	13
3.4.5 Photothermal Actuation.....	15
4. RESULTS AND DISCUSSION.....	17
4.1 Preparation of LCN Mixtures	17
4.2 Phase Transition Identification	17
4.3 Preparation of LCN Films	20
4.4 Characterization of LCN Films	21
4.4.1 Nematic LC Alignment	21
4.4.2 Order Parameter	22
4.4.3 Thermal Actuation.....	23
4.4.4 Mechanical Properties and Adaptability	26
4.4.5 Photothermal Actuation.....	31
5. CONCLUSIONS.....	35
REFERENCES.....	36

LIST OF FIGURES

Figure 1.	Composition of a liquid crystal mesogen [15].	3
Figure 2.	LC mesophases (smectic and nematic) and isotropic phase [7].	4
Figure 3.	LC monomers and crosslinked LCN [8].	5
Figure 4.	Different orientations of LC mesogens and their respective deformations (a) planar, (b) chiral nematic, (c) splay, (d) twisted nematic, and (e-f) their respective deformations [17].	6
Figure 5.	Types of formed hydrogen bonds between carboxylic groups of polyacrylic acid: (a) face on hydrogen bonds, (b) lateral hydrogen bonds [22].	7
Figure 6.	Materials used in the preparation of LC mixtures: (a) LC monomer, (b) acrylic acid, (c) azobenzene-dye (DR1), (d) crosslinker and (e) photo-initiator. Structures were drawn using chem-space.	9
Figure 7.	An image of a glass cell	11
Figure 8.	Home-made tensile testing device	15
Figure 9.	Images of LC mixtures under POM: (a) example image of LC mixtures before the phase transition, (b-i) LC mixtures at their phase transition, (b) LC-AA-0 at 67° C, (c) LC-AA-1 at 31° C, (d) LC-AA-2 at 6° C, (e) LC-AA-3 at -12° C, (f) LC-AA-4 at -24° C, (g) LC-AA-6 at -31° C, (h) LC-AA-8 at -40° C, and (i) LC-AA-10 at -41° C.	20
Figure 10.	T_{NI} values of LC-AA-0, LC-AA-1, LC-AA-2 and LC-AA-3 LC mixtures	20
Figure 11.	Images of LCN films under POM: (a, b) LCN-AA-0, (c, d) LCN-AA-1, (e, f) LCN-AA-2, (g, h) LCN-AA-3, (a, c, e, g) at 0° rotation, and (b, d, f, h) at 45° rotation. Arrows indicate the orientation of the sample	22
Figure 12.	Absorbance curves for LCN films: (a) LCN-AA-0, (b) LCN-AA-1, (c) LCN-AA-2, and (d) LCN-AA-3	23
Figure 13.	Plots of the length change percentage against the temperature for LCN films	26
Figure 14.	Stress-strain curves for LCN films in different conditions	28
Figure 15.	Changes in LCN tensile properties in dry, wet and dry-again conditions.	30
Figure 16.	Relative change of Young's modulus in wet and dry-again conditions compared to dry condition.	31
Figure 17.	Bending of splay LCN samples; before irradiation (left) and after irradiation (right).	32
Figure 18.	Changes in normalized bending angle values for LCN samples against light intensity in different conditions.	33
Figure 19.	Changes in maximum bending angle values for LCN samples in different conditions. In LCN-AA-1, the two columns for the wet condition corresponds to wet1 and wet2.	34

LIST OF TABLES

Table 1.	<i>Categories of LC materials and their information [6].</i>	4
Table 2.	<i>Materials of LC mixtures and their information.</i>	8
Table 3.	<i>Coating materials for glass slides and their parameters.</i>	10
Table 4.	<i>Different orientations obtained from coating combinations.</i>	11
Table 5.	<i>LC mixtures and the ratio of their components.</i>	17
Table 6.	<i>Polymerization temperatures for different LC mixtures.</i>	20
Table 7.	<i>Order parameter values for LCN films.</i>	23

LIST OF SYMBOLS AND ABBREVIATIONS

DA	Dry-again
DR1	Disperse red 1
LC	Liquid crystal
LCN	Liquid crystal network
POM	Polarized optical microscope
UTS	Ultimate tensile strength
UV-Vis	Ultraviolet-visible
$A_{ }$	absorbance of the sample when oriented parallel to the incident polarized light
A_{\perp}	absorbance of the sample when oriented perpendicular to the incident polarized light
E	Young's modulus
M_{AA}	molar ratio of monomer to acrylic acid
S_p	order parameter
T_{NI}	nematic-isotropic phase transition temperature
ε	tensile strain
ε_{max}	maximum tensile strain before fracture point
σ	tensile stress
σ_{max}	maximum tensile stress, or ultimate tensile strength

1. INTRODUCTION

The field of soft robotics has gained huge interest in recent years due to the versatility, flexibility, compliance and light-weight nature of its soft components compared to conventional robotics [1]. Their independence on stiff segments make them a promising platform for robotics development [2]. Soft actuators are an essential component of a soft robot, since actuators are responsible for the movement of the soft robot and its interaction with the environment [3]. A soft actuator usually depends on a stimuli-response system, where the system experiences an external stimulus such as light or heat and produce a mechanical response such as a deformation in shape [4].

Liquid crystal (LC) materials are materials that experience both liquid properties and some crystalline solid properties at a certain phase [5]. Such phase is called “liquid crystal mesophase”, and it occurs at a certain temperature called “nematic-isotropic phase transition temperature” or T_{NI} [6]. Liquid crystal networks (LCNs) are crosslinked polymer networks made of LC materials [7,8]. LCNs are considered one of the best materials for soft actuators due to their excellent properties such as high deformation ability and mechanical flexibility [9].

Photo-switches are molecules that experience photo-isomerization when irradiated by light [10]. Incorporation of such molecules into materials like LCNs makes the materials react to light stimuli, i.e., light-responsive [11]. Azobenzenes are considered one of the best types of photo-switches due to their exceptional photo-switching properties [10]. Disperse red 1 (DR1) is an azobenzene-based dye that can absorb light in the visible region [12].

The ability of LCNs to spontaneously change their mechanical properties in response to changes in the surrounding conditions, i.e., mechanical adaptability, is a crucial feature to be considered when designing an LCN-based actuator. Aquatic environments require the actuators to be more flexible and elastic than in dry land environments, due to the high drag force [13]. Therefore, a mechanically adaptable soft actuator should be capable of becoming more flexible and elastic when entering an aquatic environment and reverting back to its original properties when entering a dry land environment. One way to produce the mechanical adaptability feature is to include a secondary network within the LCN network, capable of changing its mechanical properties according to the type of

the environment. Polyacrylic acid can be used as this secondary network, since it experiences reversible hydrogen-bond-based changes when exposed to water [14].

The aim of this thesis was to investigate the effect of incorporating acrylic acid into light-responsive LCN films on the mechanical adaptability of the films when different environmental conditions were applied. This was achieved by adding the acrylic acid to the LC mixture before polymerization, and then testing the polymerized films for several parameters. First, LC mixtures were prepared with different monomer-to-acrylic-acid molar ratios (M_{AA}). Second, phase transitions were identified for all the LC mixtures and T_{NI} was determined for a selected number of the mixtures. Third, LCN films were polymerized from the best LC mixtures. Finally, LCN films were characterized via several experiments to assess their structural and mechanical properties.

The thesis is divided into five main sections including this introduction section. Section 2 is a literature review essential for the understanding of the methodology and the results of the thesis. Section 3 lists all the materials and methods used in this work. Section 4 showcases the results of the experiments, their analysis and discussion. Finally, section 5 concludes the thesis by summarizing the main points of the thesis and highlighting the impact as well as the future perspectives of this thesis.

2. LITERATURE REVIEW

This chapter highlights the main background information essential to understand the methodology, results and discussion of this work. First, an overview of liquid crystal mesophase, liquid crystals and their types is given. Second, a brief explanation of thermotropic liquid crystals, and how films synthesized from such materials behave is given. Third, photo-switches such as azobenzenes and their benefit in incorporating a light-responsive feature into thermotropic liquid crystals are introduced. Finally, the possibility of incorporating mechanical adaptability to liquid crystal films is discussed via adding certain compounds such as acrylic acid.

2.1 Liquid Crystal and Liquid Crystal Materials

LC mesophase is an intermediate phase occurring between the isotropic liquid phase and anisotropic crystalline solid phase, experienced by materials called "LC materials" [5]. At LC mesophase, LC materials have liquid-like flow and fluidity, resulting in isotropic properties but their building units are somewhat ordered, resulting in some crystalline solid (anisotropic) properties [5,6]. The building units of LC materials are rigid molecules called "mesogens", where each mesogen consists of a stiff rod-like or disk-like backbone core, flexible spacers and polymerizable end groups, as illustrated in Figure 1 [15].

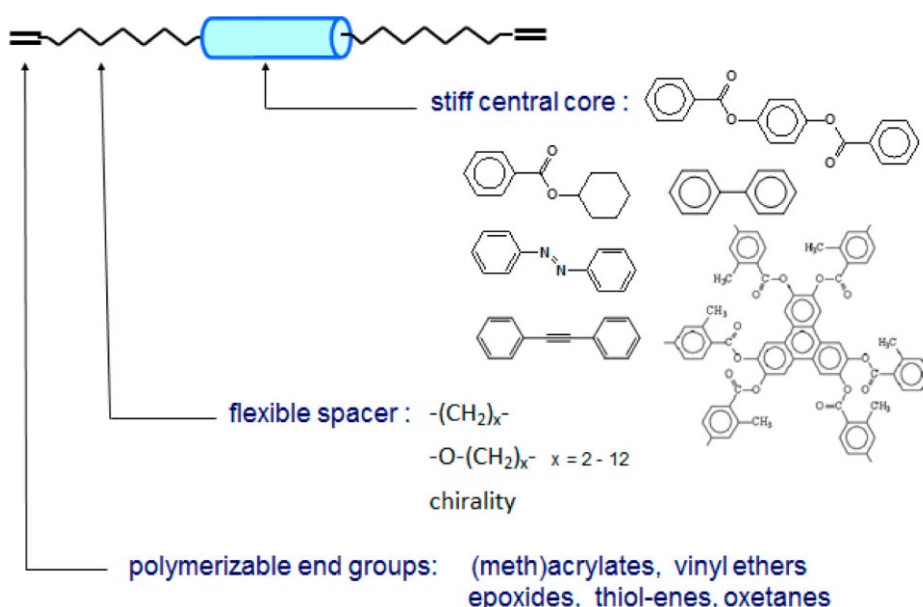


Figure 1. Composition of a liquid crystal mesogen [15].

Within the LC mesophase, there exist other mesophases, most notably nematic and smectic mesophases, where they differ on the type of their orientational order and the

order of the mesogens' centers of mass [5]. In both the nematic and smectic phases, the orientation of the mesogens is in one direction, however, the nematic phase does not have periodicity, while the smectic phase is characterized by mesogens being aligned in layers with some periodicity [5,16]. The difference between nematic and smectic mesophases in comparison to the isotropic phase is illustrated in Figure 2. LC materials are characterized by their ability to transition between the isotropic phase and the LC mesophases in a reversible manner depending on the temperature [6,16]. This work focuses specifically on the nematic mesophase and the transition between this phase and the isotropic phase. That transition from isotropic to nematic LC mesophase occurs at a specific temperature T_{NI} [6].

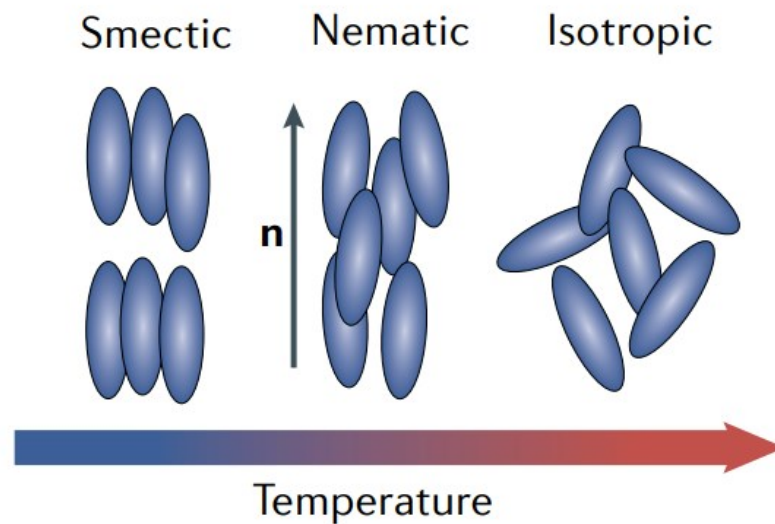


Figure 2. LC mesophases (smectic and nematic) and isotropic phase [7].

LC materials have several categories: (1) thermotropic, (2) lyotropic, and (3) metallotropic, where they differ depending on the composition of their mesogens and the factors affecting the phase transition as shown in Table 1 [6]. This work focuses on thermotropic LC materials and their networks, therefore, temperature will be an important factor in this thesis.

Table 1. Categories of LC materials and their information [6].

LC Material	Chemical Composition	Factors Affecting T_{NI}
Thermotropic	Organic mesogens	<ul style="list-style-type: none"> • Temperature
Lyotropic	Amphiphilic mesogens dissolved in a solvent	<ul style="list-style-type: none"> • Temperature • Concentration of mesogens
Metallotropic	Organic and Inorganic mesogens	<ul style="list-style-type: none"> • Temperature

		<ul style="list-style-type: none"> • Concentration of mesogens • Composition ratio of organic to inorganic mesogens
--	--	---

2.2 Thermotropic Liquid Crystal Networks

LCNs are crosslinked polymer networks that are composed of liquid crystal mesogens, as illustrated in Figure 3 [7,8]. Thermotropic LCNs are LCNs made from thermotropic liquid crystals. When a thermotropic LCN gets stimulated by heat and reaches T_{NI} , the phase transition still occurs but in the form of order reduction that consequently results in the deformation of the LCN's shape or size [7].

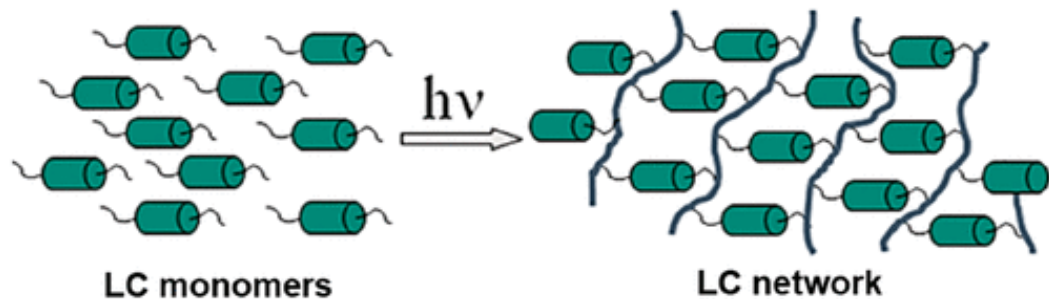


Figure 3. LC monomers and crosslinked LCN [8].

The type of deformation depends on the type of the mesogens' orientation, where each orientation causes its unique shape deformation when stimulated, as illustrated in Figure 4 [17]. Therefore, LCNs are usually used as soft actuators due to their motor abilities that can be triggered by external stimuli such as heat [8]. In the next section, we discuss how to trigger LCNs using light instead of heat.

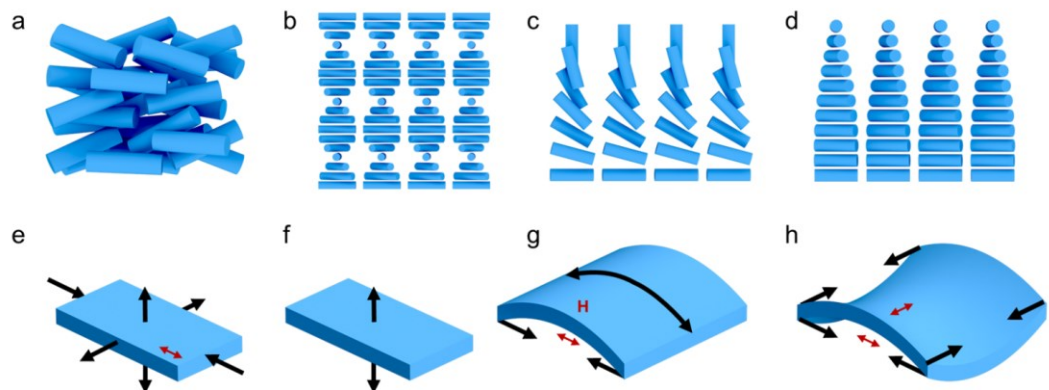


Figure 4. *Different orientations of LC mesogens and their respective deformations (a) planar, (b) chiral nematic, (c) splay, (d) twisted nematic, and (e-f) their respective deformations [17].*

2.3 Light Responsivity

Photo-switches or photo-switchable molecules are molecules that experience photo-isomerization (trans to cis) when irradiated by light [10]. Incorporation of such molecules into materials makes the materials react to light stimuli, i.e., light-responsive [11]. They have been widely used in several applications such as optical devices and smart polymeric systems [18]. One of the most interesting types of photo-switches in research are azobenzenes, due to their exceptional photo-switching properties [10]. DR1 is an azobenzene-based dye that has two absorption bands, between 260 and 310 nm in the UV region and between 360 and 590 nm in the visible region [12].

Light-responsive deformation of LCNs through azobenzenes can occur via two mechanisms of actuation: (1) photochemical actuation and (2) photothermal actuation. In photochemical actuation, the azobenzenes are crosslinked or grafted chemically into the LCN polymer chains [19]. Upon exposure to light, the photo-isomerization of the azobenzenes from trans to cis will build stress in the network, causing the network to deform in shape [20]. The time duration of the deformation is dependent on the lifetime of the cis-isomer of the azobenzene in question [19]. In photothermal actuation, the azobenzenes are physically incorporated in the LCN network either before or after polymerization. Unlike photochemical actuation, photothermal actuation relies on the conversion of light energy to heat through rapid photo-isomerization of the azobenzenes [19]. That generated heat will then stimulate the phase transition of LCNs, and deformation occurs [21]. Since photothermal induction requires rapid photo-isomerization, azobenzenes with short cis-isomer lifetime such as DR1 and its derivatives are used [21]. In this thesis, DR1 was incorporated via physically blending it with the rest of the LC components before polymerization to prepare photothermal light-responsive LCNs.

2.4 Mechanical Adaptability

One of the crucial features of smart soft robotics is their ability to adapt to various environmental conditions. An important type of adaptability is the ability of the LCN-based actuators to spontaneously change their mechanical properties in response to changes in their environment, i.e., mechanical adaptability. Aquatic environments, where interaction with water is inevitable, requires the actuators to be more flexible and elastic than in

dry land environments, due to the high drag force [13]. Therefore, a mechanically adaptable LCN-based actuator should be capable of fully functioning in both environments, where it becomes more flexible and elastic when entering an aquatic environment and reverts back to its original properties when entering a dry land environment.

The key to implementing this mechanical adaptability feature is to use a compound that experiences reversible structural changes when exposed to water. Polyacrylic acid is considered to be a good candidate in such application. Polyacrylic acid forms hydrogen bonds between its own units in dry conditions (illustrated in Figure 5) but breaks those bonds and forms other hydrogen bonds with water molecules when exposed to water [14]. Different techniques of implementations can be considered. One way is to have acrylic acid chemically bound to the backbone of the LCN polymer chain or to have one of the LCN components possessing the same functional groups as in acrylic acid (free carboxylic groups). Another way is to include a secondary network made of polyacrylic acid within the LCN network, where this secondary network is responsible for the mechanical adaptability. The latter way is used via physically blending acrylic acid with the LC mixture before polymerization. In this thesis, acrylic acid was incorporated into the LCNs using the latter way.

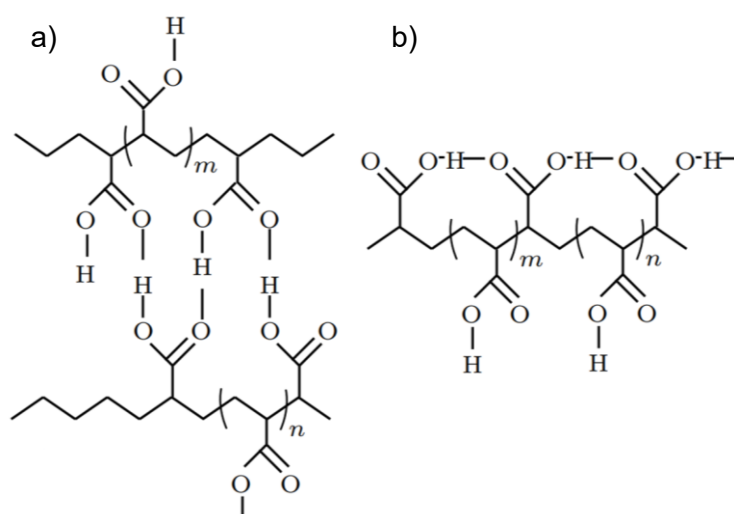


Figure 5. Types of formed hydrogen bonds between carboxylic groups of polyacrylic acid: (a) face on hydrogen bonds, (b) lateral hydrogen bonds [22].

3. MATERIALS AND METHODS

This chapter introduces the materials used in this thesis and how they were used to prepare the LC mixtures and films. Moreover, this chapter explains the methods used for the preparation and characterization of the LC mixtures and films. Preparation and characterization of the LC mixtures and films were done according to the most up-to-date protocols found in literature.

3.1 Preparation of LC Mixtures

The materials used in this part and their information are listed in Table 2 and illustrated in Figure 6. LC mixtures were prepared from the first three components (1) LC monomer, (2) crosslinker, (3) azobenzene-based dye. Acrylic acid was added with varied values of M_{AA} . The photo-initiator was added later during the film preparation section and was not added during this part to prevent unwanted polymerization. To prepare the LC mixture, the needed amount of each material was weighed and added to a 7-ml amber glass vial. The glass vial was then put in a water bath at 70 °C while magnetically stirring at around 500 rpm for few minutes until the mixture is completely melted and homogenous.

Table 2. *Materials of LC mixtures and their information.*

Liquid Crystal Component	Chemical Name	Molecular Formula	Molecular Weight (g/mol), (Quality)	Supplier
LC Monomer	4-Methoxybenzoic acid 4-(6-acryloyloxy-hexyloxy)phenyl ester	C ₂₃ H ₂₆ O ₆	398.45, (97%)	SYNTHON Chemicals GmbH & Co. KG
Crosslinker	1,4-Bis[4-(6-acryloyloxyhexyloxy)benzyloxy]-2-methylbenzene	C ₃₉ H ₄₄ O ₁₀	672.76, (97%)	SYNTHON Chemicals GmbH & Co. KG
Azobenzene-based dye	<i>N</i> -Ethyl- <i>N</i> -(2-hydroxyethyl)-4-(4-nitrophenylazo)aniline	C ₁₆ H ₁₈ N ₄ O ₃	314.34, (95%)	Sigma-Aldrich
Mechanical Adaptable Compound	Acrylic acid (Propenoic acid)	C ₃ H ₄ O ₂	72.06, (99%)	Sigma-Aldrich
Photo-initiator	2,2-Dimethoxy-2-phenylacetophenone	C ₁₆ H ₁₆ O ₃	256.30, (99%)	Sigma-Aldrich

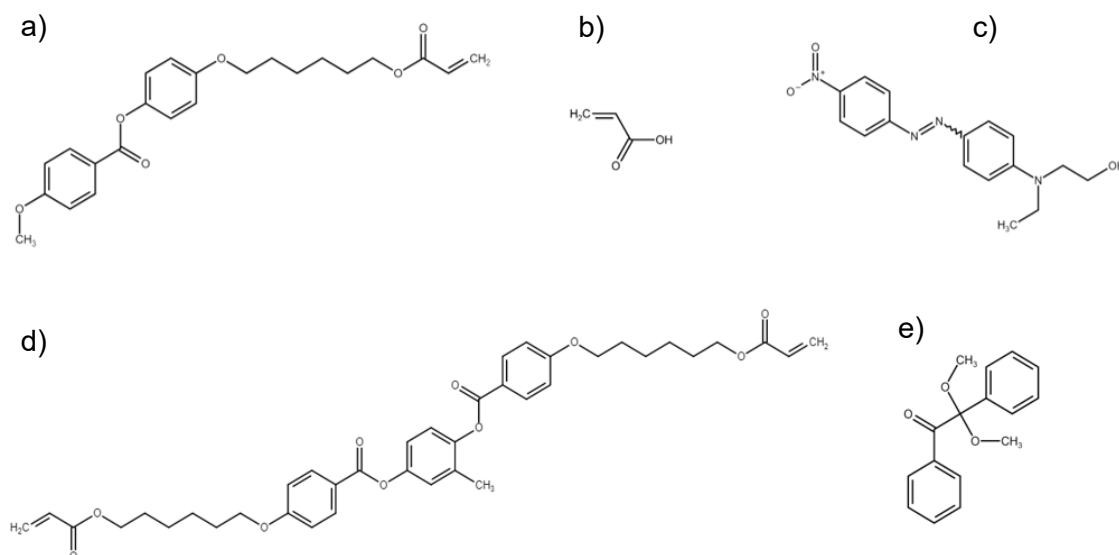


Figure 6. Materials used in the preparation of LC mixtures: (a) LC monomer, (b) acrylic acid, (c) azobenzene-dye (DR1), (d) crosslinker and (e) photo-initiator. Structures were drawn using chem-space.

3.2 Phase Transition Identification

Phase transition was identified for the LC mixtures using Polarized Optical Microscope (POM) ZEISS Axio Imager 2 (Carl Zeiss AG) and attaching a heating/cooling THMS350 stage (Linkam Scientific Instruments Ltd.). A liquid nitrogen tank was attached to the stage to support low temperatures that cannot be attained by the stage alone. The LC mixture was heated on a 70 °C while magnetically stirring at around 500 rpm for few minutes to ensure the complete melting and homogeneity of the mixture. A drop of the LC mixture was added between two microscope coverslips (22x22mm, Thermo Fisher Scientific Inc.). Excess mixture was gently removed from the edges using a paper towel and then the whole sample was put on the stage. Nitrogen flush was used on the sample while being covered with an acrylate lid to prevent the formation of frost at low temperatures. Two polarizers were installed, where one was at 0° and the other was at 90°, which results in a dark image. The temperature was increased to 70 °C at a high rate (20 or 30 °C/min), then decreased at a rate of 1-5 °C/min, while maintaining each temperature point for around 1 minute before proceeding to the next temperature point. The temperature was decreased until a change in the texture of the sample was observed. The change was the appearance of small red particles throughout the whole sample. It is worth noting that reducing the range of the measurement for less time-consumption was possible by first using high temperature rates (around 20 °C/min) in cooling until observing the transition, then back-tracking few degrees Celsius and repeating the same procedure with the lower rates (1-5 °C/min), where in this case, the starting point can be

closer to the transition point. After identifying the transition point, snapshots were taken before and after that point using ZEN Microscopy Software (Carl Zeiss AG). The same procedures were conducted on each LC mixture prepared. Moreover, T_{NI} was determined for selected LC mixtures and plotted using OriginLab software program (OriginLab Corporation).

3.3 Preparation of LCN Films

To synthesize LCN films, glass cells were prepared using microscopic glass slides (3x1 inch, Thermo Fisher Scientific Inc.). Each slide was cut into two smaller slides, 1-inch slide and 2-inch slide. The glass slides were cleaned using Elmasonic P30H sonication device (Danbrit Oy) in two steps: (1) in acetone for 20 minutes, and (2) in 2-propanol for 20 minutes. For both steps, the frequency of sonication was 80 Hz, and the temperature was not adjusted. The glass slides were then placed on a paper towel for a few minutes to dry, while avoiding flipping the slides to prevent contaminating the other side with the paper towel. Glass slides were cleaned using compressed nitrogen to remove any dust accumulated during the drying process. Each slide was put in WS-650-23NPPB Spin Coater (Laurell Technologies Corporation), and few drops of one of the coating materials listed in Table 3 were added on top of the slide using a Pasteur pipette and spread evenly on the slide surface using the pipette tip. Polyvinyl alcohol (PVA) solution (5% w/w) was prepared by adding 5% (of the total weight) PVA (98-99% hydrolyzed, Sigma-Aldrich) and distilled water for the rest 95%. The mixture was then put in an oil bath at 90 °C for around 30 minutes until complete dissolution. Polyimide materials (JSR Micro NV) were directly used from their containers. The spin-coating parameters and the need for rubbing after spin-coating were different depending on the coating material as shown in Table 3.

Table 3. *Coating materials for glass slides and their parameters.*

Coating Material	Spin-coating Parameters	Rubbing
Polyvinyl Alcohol Solution (5% w/w)	4000 rpm, 1 minute	Yes
Polyimide OPTMER AL 1254	2000 rpm, 1 minute	Yes
Polyimide OPTMER AL 60101L	5000 rpm, 1 minute	No

After spin-coating, the PVA-coated slides were put on a heat plate at 90 °C for 5 minutes while the polyimide-coated slides were put on a heat plate at 90 °C for 1 minute, then at 180 °C for 20 minutes. Heating at 90 °C was to evaporate the solvent from the PVA solution and the polyimide materials, and heating at 180 °C was to cure the polyimide

materials. The rubbing process was done manually, where each slide was fixed on a stage and a satin fiber was used to rub the slide in one direction (not back and forth) parallel to the cut edge of the slide. The slides were then cleaned using compressed nitrogen to remove any dust or fiber particles. The final step to prepare the glass cell was to glue two slides together. The combination of the coated slides was chosen depending on the orientation of the mesogens needed as listed in Table 4. Spacers made of dry borosilicate glass microspheres (5 and 50 μm , Thermo Fisher Scientific Inc.) were used to adjust the thickness of the glass cell. Little amounts of UVS 91 glue (Norland Products, Inc) and the spacers were mixed, a small amount of that mixture was added on each corner of the top slide, and the top slide was then put on the other slide as shown in Figure 7. The two slides together were irradiated with UV light via either pE-4000 (365 nm, 0.44 W, CoolLED Limited), or M375L3 (375 nm, 387 mW, Thorlabs, Inc) for 1 minute to cure the glue.

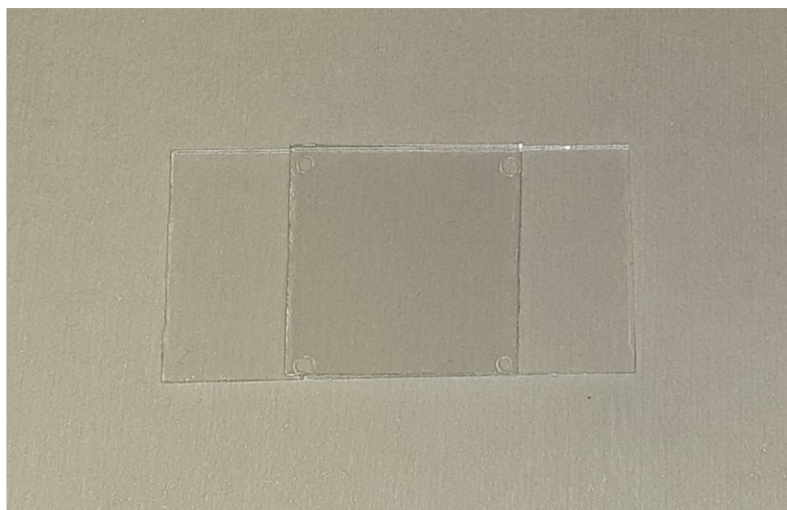


Figure 7. An image of a glass cell

Table 4. Different orientations obtained from coating combinations.

Coating of the First Slide	Coating of the Second Slide	Orientation
Polyvinyl Alcohol (PVA) Solution (5% w/w)	Polyimide OPTMER AL 1254	Planar
Polyvinyl Alcohol (PVA) Solution (5% w/w)	Polyimide OPTMER AL 60101L	Splay

To prepare the LC mixture for polymerization, a photo-initiator (1% of the total weight) was added to the mixture and stirred magnetically at 70 °C until complete homogeneity. The photo-initiator was chosen depending on the wavelength that will be used during polymerization, in this case 365 nm. Moreover, from the point of adding the photo-initiator, red light was used for the rest of the polymerization process to prevent the activation

of the photo-initiator before the actual process. The glass cells were added on the heat plate at 70 °C with the LC mixture, and the LC mixture was added on the edge of the cell using a micropipette. The cells were filled with the mixture via capillary suction. When all the cells were filled completely, each one was transported to the polymerization stage while maintaining its 70 °C temperature using a thick metal plate. The polymerization stage was composed of a heating/cooling LTS120 stage (Linkam Scientific Instruments Ltd.), supplied with EHEIM Professional 3 water thermofilter (Eheim GmbH & Co. KG). The cells were then cooled down from 70 °C to the polymerization temperature of the LC mixture in question at a rate of 5-20 °C/min. Higher rates were used to skip temperature points when the polymerization temperatures were very low. For example, if the polymerization temperature is -6 °C, then the temperature was cooled from 70 °C to 20 °C at a rate of 20 °C/min, then from 20 °C to -6 °C at a rate of 5 °C/min. If the polymerization temperature was very low, the acrylate lid with the nitrogen flush were used as in section 3.2 to prevent frost formation. After the cell had reached the polymerization temperature, the cell was radiated with pE-4000 (365 nm, 0.44 W, CoolLED Limited) for 5 minutes. The cells were then opened using a razor blade while some cells needed to be kept in a warm water bath (less than 60 °C) for 1-2 days before opening them.

3.4 Characterization of LCN Films

This section introduces the methodology used for the characterization of LCN films. Each method, and how they were used to measure several parameters of the LCN films are explained thoroughly.

3.4.1 Nematic LC Alignment

The quality of the nematic LC alignment was observed using similar setup to the one in section 3.2 but with a normal stage not the heating/cooling stage. 5- μm -thick planar LCN films were used for this section, where each film was put on the POM stage, 5x lens was used, and the stage was rotated 45° (clockwise or anticlockwise). A snapshot image was taken before the rotation and after using ZEN Microscopy Software to observe the contrast between the two images.

3.4.2 Order Parameter

The quality of the nematic LC alignment can also be assessed by calculating the order parameter for the LCN film. Order parameter can be determined for LCN samples using the following equation:

$$S_p = \frac{A_{||} - A_{\perp}}{A_{||} + 2A_{\perp}}, \quad (1)$$

where S_p is the order parameter, $A_{||}$ is the absorbance of the sample when it is oriented parallel to the incident polarized light, and A_{\perp} is the absorbance of the sample when it is oriented perpendicular to the incident polarized light. 5- μm -thick planar LCN films in their respective glass cells were used for this section, where each film's absorbance in both directions were measured using Cary 60 UV-Visible (UV-Vis) Spectrophotometer (Agilent Technologies). The range of the spectrum was 350-600 nm, and the slow option was used. Two microscopic glass slides were used to act as a blank cell for the zero reference of the measurements. Equation (1) was used at different points of the spectrum, near the extremes where there were less fluctuations. The order parameter calculated from these different data points were then averaged using MS Excel. Moreover, the curves of the absorbance spectra were plotted against the wavelength using OriginLab.

3.4.3 Thermal Actuation

Thermal actuation of the LCN films was assessed using the same setup in section 3.2. This test was used to assess the absolute contraction of the LCN film and their recovery capacity. 50- μm -thick planar LCN films were used, where a small rectangular piece (around 1.5x0.5 mm) was cut along the alignment direction. Few drops of distilled water were added on the film to loosen the pieces and extract them from the film. The pieces were then dried on a hot plate at 100 °C for few minutes. Little amounts of 50- μm spacers were added on the surface of a microscope coverslip (22x22mm, Thermo Fisher Scientific Inc.), then the cut piece was added on the top. This was done to prevent the piece from sticking to the surface during the test. The slide was then placed on the stage and the 5x lens was used. The temperature was raised from 30 °C to 120 °C and then cooled down to 30 °C in 10 °C steps at a rate of 10 °C/min. After reaching each temperature point, the temperature was maintained for at least 1 minute, and a snapshot image was taken before proceeding to the next temperature point. Moreover, each snapshot was further processed through manually measuring the length of the piece using the length measuring tool in ZEN Microscopy Software. The relative change in length was then plotted against the temperature using OriginLab.

3.4.4 Mechanical Properties and Adaptability

The mechanical properties of the LCN films and their adaptability to different surrounding conditions were assessed using the tensile testing device illustrated in Figure 8. The tensile testing device was a home-made device, composed of the following: (1) KD34s

force sensor (± 5 , ME-Meßsysteme GmbH), (2) GSV-2TSD-DI measuring amplifier for the sensor (ME-Meßsysteme GmbH), and (3) M-403 linear stage (Physik Instrumente GmbH & Co. KG). 50- μm -thick planar LCN films were used, where stripes (25x1 mm) were cut along the alignment direction. Few drops of distilled water were added on the film to loosen the stripes and extract them from the film. The stripes were dried on a hot plate at 100 °C for few minutes. After that step, three conditions were used: (1) dry condition, (2) wet condition, and (3) dry-again (DA) condition. The dry condition was achieved by using the stripes directly. The wet condition was achieved by immersing the stripes in water (distilled water and/or tap water) for 5 minutes. The dry-again condition was achieved by immersing the stripes in water (similar to the wet condition), then drying them on a hot plate at 100 °C for few minutes. It is worth noting that performing the test underwater was initially decided but due to the device's inability to perform underwater, it was decided to have the wet condition as an alternative. Three samples were used for each film in each condition, making them nine samples for each film type. The stripes were then attached to a paper frame and inserted between the clamps of the tensile testing device. The starting distance between the two clamps was 12.76 mm, and the speed of the stretching used was 0.1 mm/sec. The test was conducted until the fracture point of the stripes. Data points of stress (σ) and strain (ϵ) were then produced, and they were plotted against each other. Maximum strain (ϵ_{max}) was determined by measuring the maximum value of tensile strain for each sample before fracture point. Ultimate tensile strength (UTS or σ_{max}) was determined by measuring the maximum value of tensile stress for each sample. Young's modulus (E) was determined by calculating the slope of the linear region of the stress-strain curve. Average values of ϵ_{max} , σ_{max} and E were plotted against the type of condition to visualize the change in the mechanical strength of the LCN films between different conditions. Moreover, in order to quantify the extent of the change in the mechanical properties and the quality of their recovery, percentage values of the relative change in Young's modulus in wet and dry-again conditions compared to dry condition were calculated and plotted. The calculations were done using MS Excel, and the plots were produced using OriginLab.

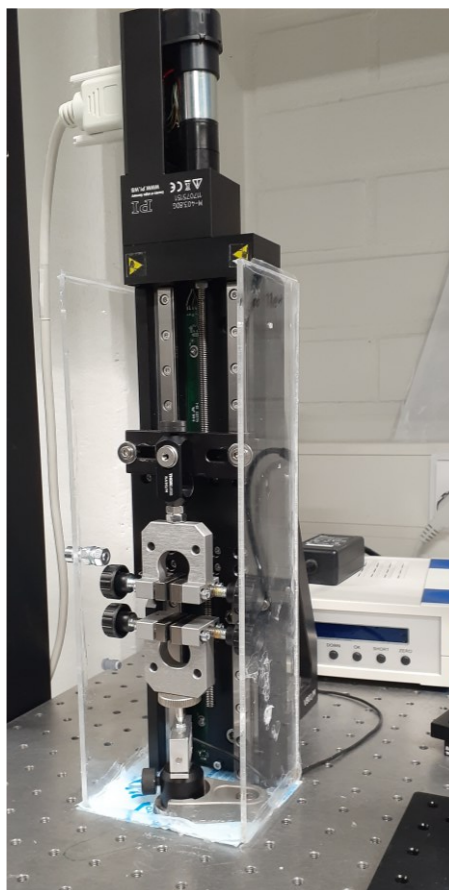


Figure 8. Home-made tensile testing device

3.4.5 Photothermal Actuation

The light responsivity of the LCN films were assessed using a bending-tracking test. 50- μm -thick splay LCN films were used, where stripes (6x1 mm) were cut along the alignment direction. Similar to section 3.4.4, the same three conditions were investigated (dry, wet and dry-again). However, the same LCN sample was used for the three conditions, since the sample was not damaged at the end of the measurement. Similar to the previous section, performing the test underwater was limited but in this case, it was because the light energy dissipates in water before stimulating the sample. At wet condition, excess water was gently removed from the samples with a paper towel to prevent the extra weight of water from hindering the bending extent of the stripes. Each LCN sample was fixed at a distance 3-4 cm from the pE-4000 light source. The sample was then radiated with 460 nm blue light at full power (0.61 W) to anneal the sample, so that any pre-stress stored in the film was removed. After the annealing was done, the initial angle before the starting the test was measured. The test started by using 10% power (100 mW) until 100% in 10% increments. At each step, the light was maintained at on and off states for few seconds to ensure that the film could reach equilibrium at both states. The test was done for the three samples in the three conditions. All the tests were videotaped for

analysis of the bending angle of the LCN samples in the three conditions. The analysis was done using Kinovea video annotation software program, where the angle was manually measured using the angle tracking tool. The bending angles were normalized by subtracting their respective initial angle from them. These normalized angle values were then plotted against the light intensity. Moreover, in order to quantify the extent of the change in the final bending angle, percentage values of the relative change in the final bending angle in wet and dry-again conditions compared to dry condition were calculated and plotted. The calculations were done using MS Excel, and the plots were produced using OriginLab.

4. RESULTS AND DISCUSSION

This chapter showcases the results of the measurements and tests conducted on LCNs, as well as their analysis and discussion. These include the preparation of the LCN mixtures and their phase transition, and the preparation of the LCN films and their characterization.

4.1 Preparation of LCN Mixtures

Eight LC mixtures were prepared based on the ratio of the monomer to the acrylic acid shown in Table 5. The amounts of the azobenzene-based dye and the photo-initiator were fixed as 1% of the total weight for each. The mixtures were named based on this template “LC-AA-1/ M_{AA} ”. For example, the LC mixture with an M_{AA} of 1:2 is named LC-AA-2. Moreover, LC-AA-0 was prepared as the control mixture where no acrylic acid was added.

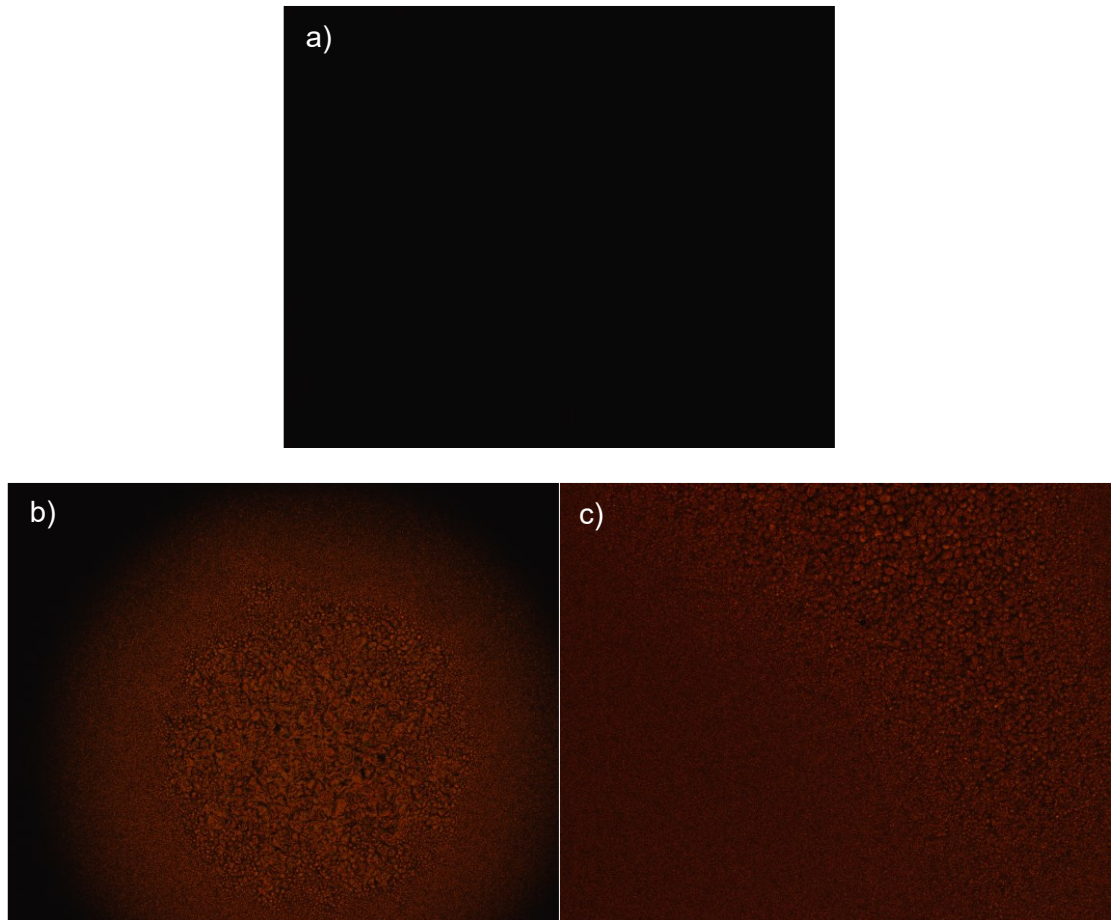
Table 5. LC mixtures and the ratio of their components.

LC Mixture	Monomer-to-Acrylic-Acid Molar Ratio (M_{AA})	Crosslinker-to-Monomer-to-Acrylic-Acid Molar Ratio
LC-AA-0	1:0	1:5:0
LC-AA-1	1:1	1:5:5
LC-AA-2	1:2	1:5:10
LC-AA-3	1:3	1:5:15
LC-AA-4	1:4	1:5:20
LC-AA-6	1:6	1:5:30
LC-AA-8	1:8	1:5:40
LC-AA-10	1:10	1:5:50

4.2 Phase Transition Identification

Phase transition was identified for the LC mixtures using POM. Figure 9 shows the contrast between two states, right before reaching the phase transition (black image) and after reaching that transition for the eight LC mixtures. However, not all the transitions were nematic-isotropic transitions. From LC-AA-4 till LC-AA-10, the phase transition

was observed to be less smooth than in the rest of the LC mixtures. This can be attributed to acrylic acid disturbing the nematic LC alignment of the mixtures until reaching a point where it causes the material to transition from the isotropic phase directly to the anisotropic (solid crystalline) phase and skipping the LC phase completely. Therefore, the phase transition temperatures were identified as T_{NI} only for LC-AA-0, LC-AA-1, LC-AA-2, and LC-AA-3. T_{NI} was observed to be decreasing as M_{AA} decreased as shown in Figure 10., which means that increasing the amount of acrylic acid in the LC mixture causes T_{NI} to decrease. For the following sections, it was decided to proceed with LC-AA-0, LC-AA-1, LC-AA-2, and LC-AA-3.



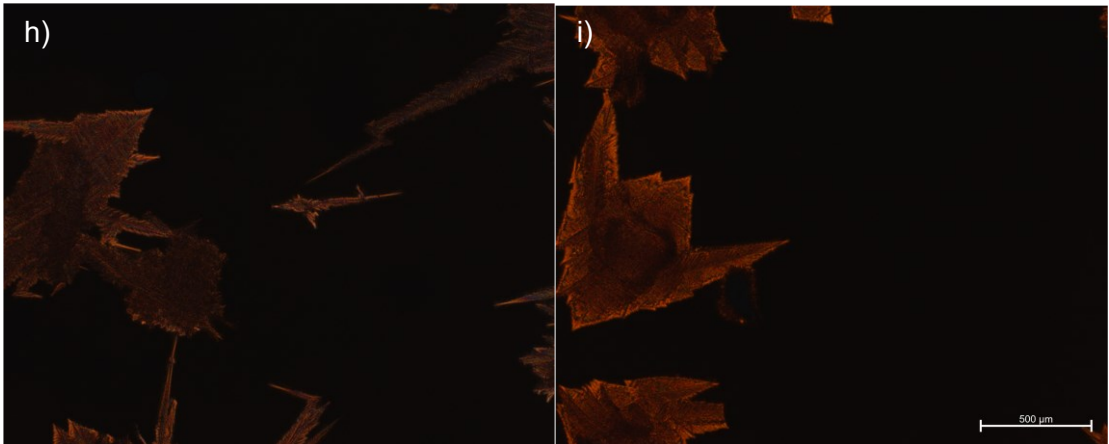
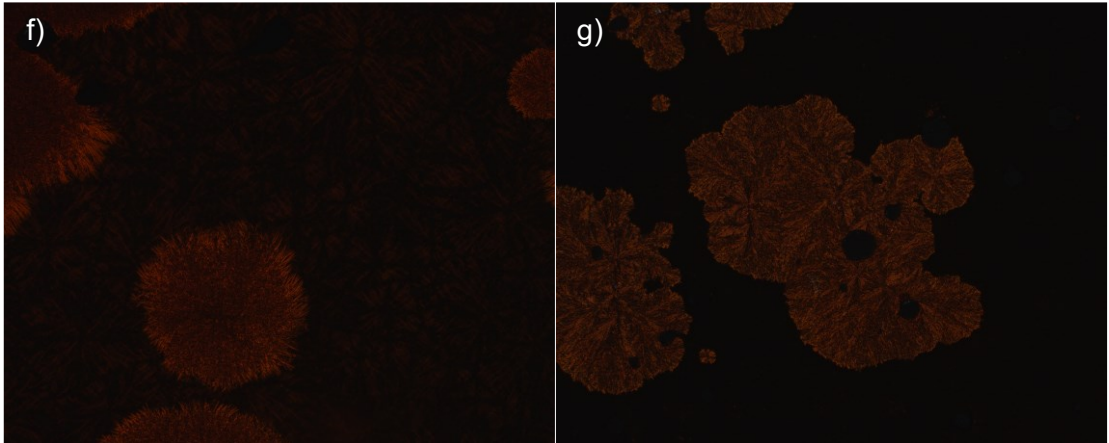
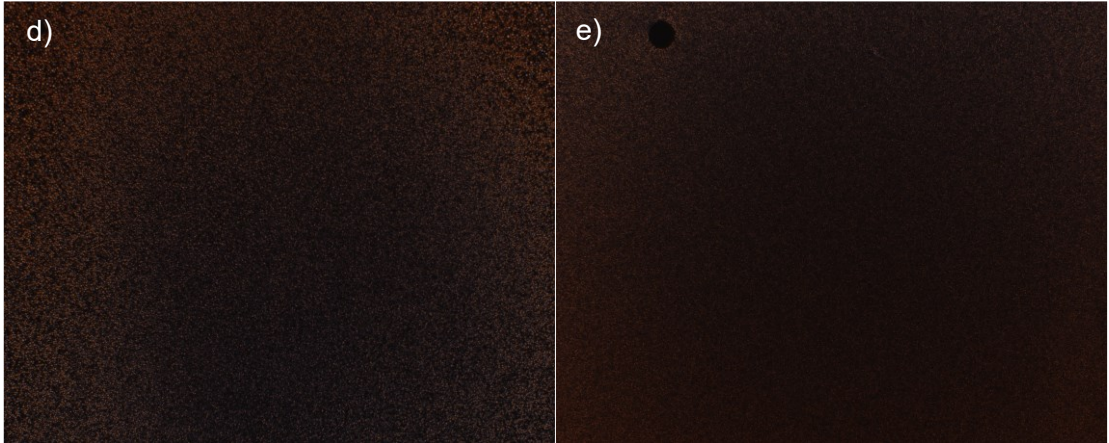


Figure 9. Images of LC mixtures under POM: (a) example image of LC mixtures before the phase transition, (b-i) LC mixtures at their phase transition, (b) LC-AA-0 at 67° C, (c) LC-AA-1 at 31° C, (d) LC-AA-2 at 6° C, (e) LC-AA-3 at -12° C, (f) LC-AA-4 at -24° C, (g) LC-AA-6 at -31° C, (h) LC-AA-8 at -40° C, and (i) LC-AA-10 at -41° C.

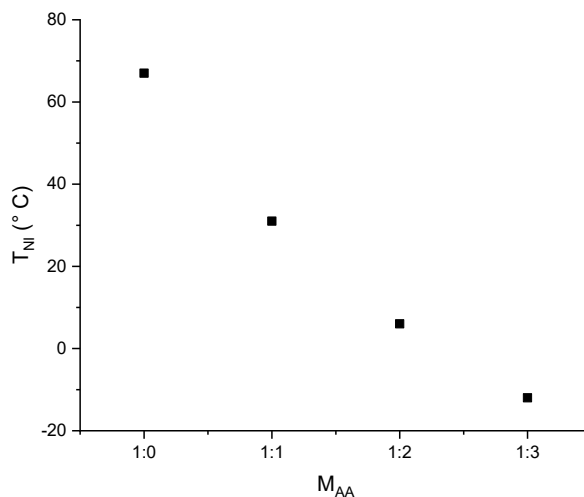


Figure 10. T_{NI} values of LC-AA-0, LC-AA-1, LC-AA-2 and LC-AA-3 LC mixtures

4.3 Preparation of LCN Films

LCN films were prepared from the first four LC mixtures, because films prepared from mixtures with higher acrylic acid content could not maintain decent alignment. The naming system of the LCN films was the same as with the mixtures, except for replacing “LC” with “LCN” to indicate the formation of the network. The polymerization temperatures used for LC mixtures were calculated by subtracting 12 °C from the LC phase transition temperature of the LC mixture as illustrated in Table 6.

Table 6. Polymerization temperatures for different LC mixtures.

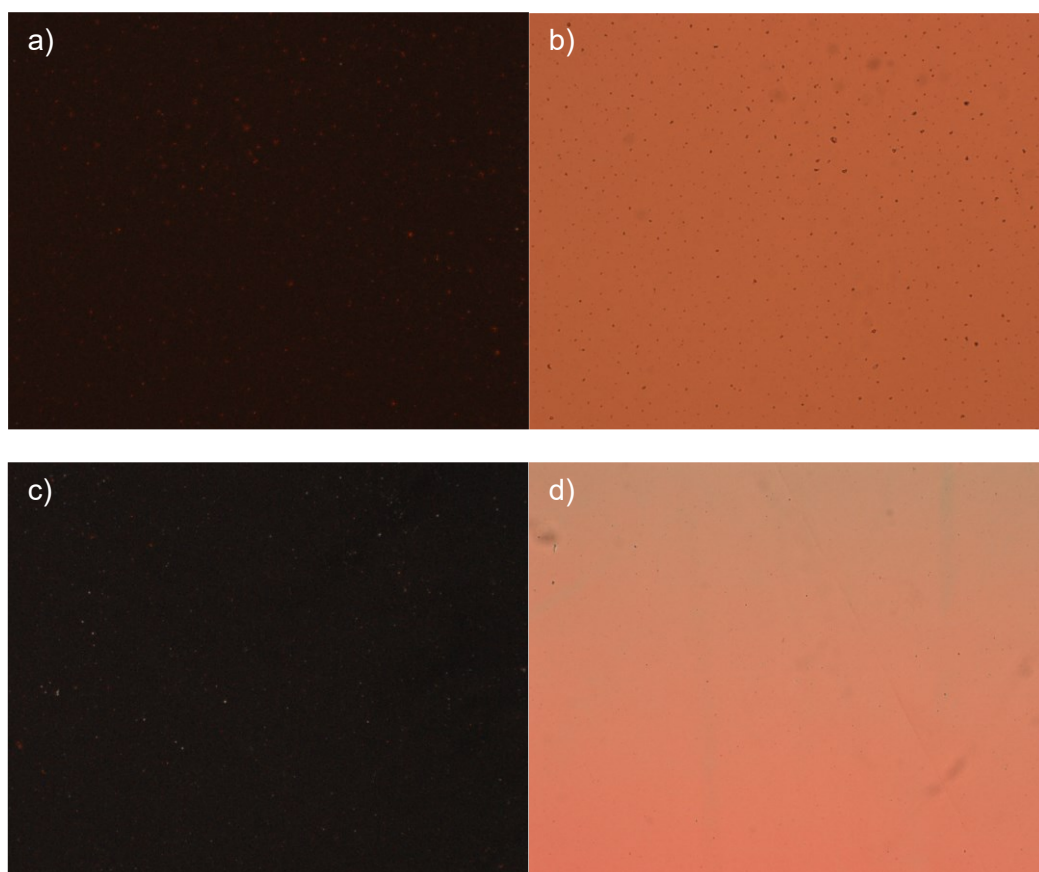
LC Mixture	T _{NI}	Polymerization Temperature
LC-AA-0	67 °C	55 °C
LC-AA-1	31 °C	19 °C
LC-AA-2	6 °C	-6 °C
LC-AA-3	-12 °C	-24 °C

4.4 Characterization of LCN Films

In this section, LCN films characterization results and their analysis are shown. Order parameter and nematic alignment tests were used to assess the quality of the LCN films alignment. Thermal actuation test was used to assess the contraction of the LCN films in response to heat. Mechanical properties and adaptability tests were used to assess the mechanical strength of the LCN films and how they can change depending on the environment of the films. Photothermal actuation test was used to assess the light responsiveness of LCN films in different conditions.

4.4.1 Nematic LC Alignment

The nematic LC alignment of mesogens was observed using POM. Figure 11 shows the contrast between the 0° state and the 45° state for the four mixtures. It was observed that the contrast between the two states is decreasing as M_{AA} decreased, supporting the same claims mentioned in section 4.2 and 4.4.1.



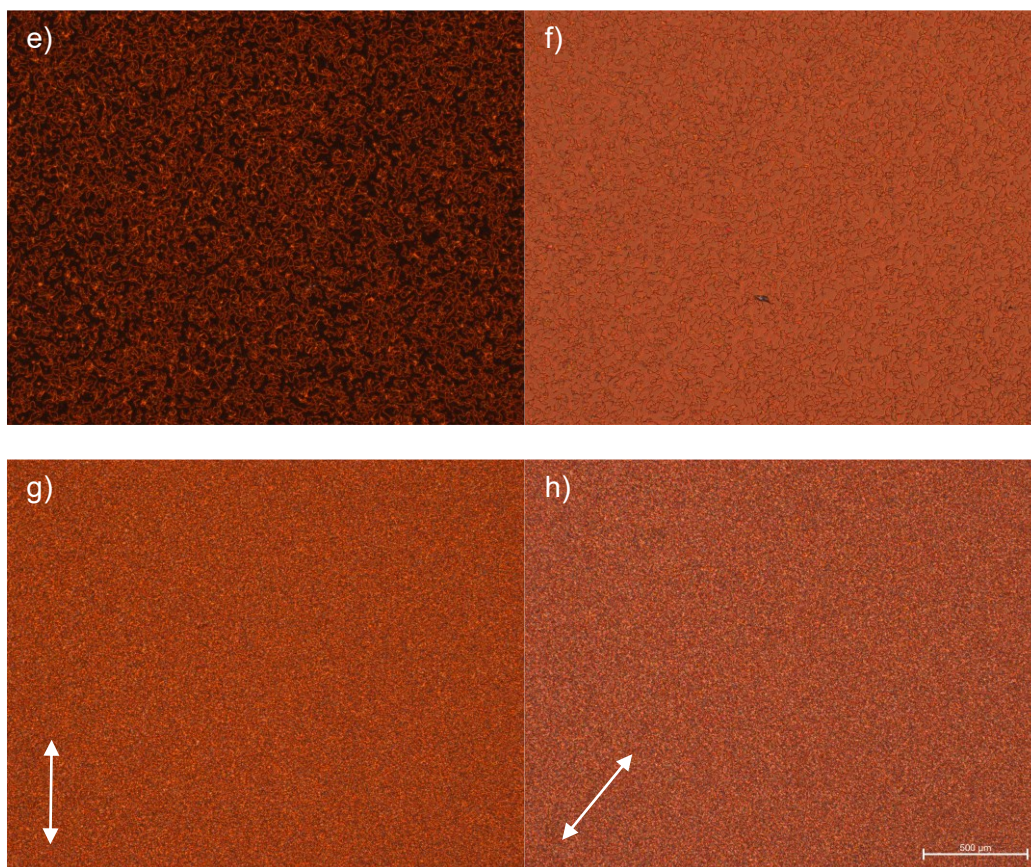
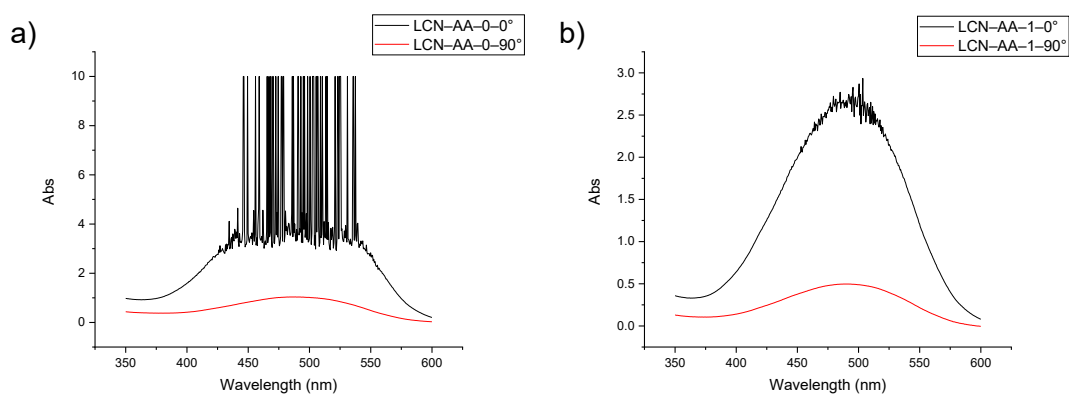


Figure 11. Images of LCN films under POM: (a, b) LCN-AA-0, (c, d) LCN-AA-1, (e, f) LCN-AA-2, (g, h) LCN-AA-3, (a, c, e, g) at 0° rotation, and (b, d, f, h) at 45° rotation. Arrows indicate the orientation of the sample

4.4.2 Order Parameter

Order parameter for the synthesized films was calculated using equation (1). Figure 12 shows the absorbance curves for the films produced from UV-Vis spectrophotometer. The overshooting in some of the curves is due to the limitations of the UV-Vis spectrophotometer, where it registers absorbance measurements above certain values as an overshoot.



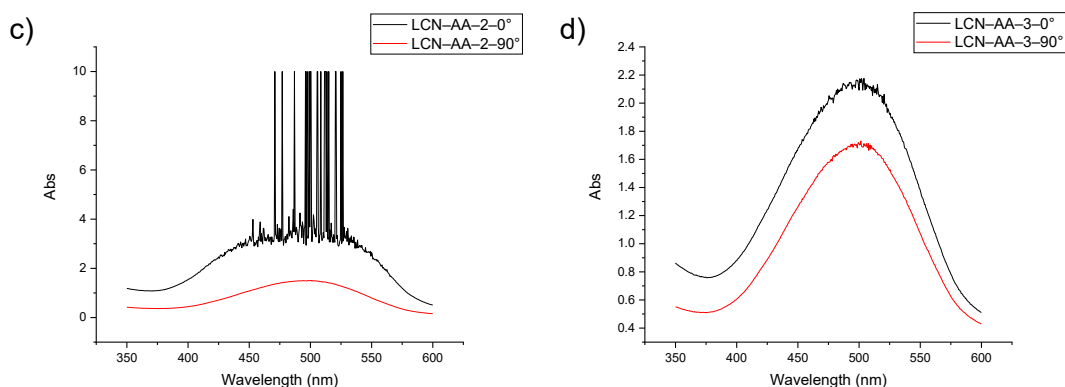


Figure 12. Absorbance curves for LCN films: (a) LCN-AA-0, (b) LCN-AA-1, (c) LCN-AA-2, and (d) LCN-AA-3

Table 7 lists the order parameter values of the four LCN film, where the order parameter was observed to be decreasing as the acrylic acid content increases. This supports previous claims in section 4.2 that higher acrylic acid content interferes with the alignment of mesogens.

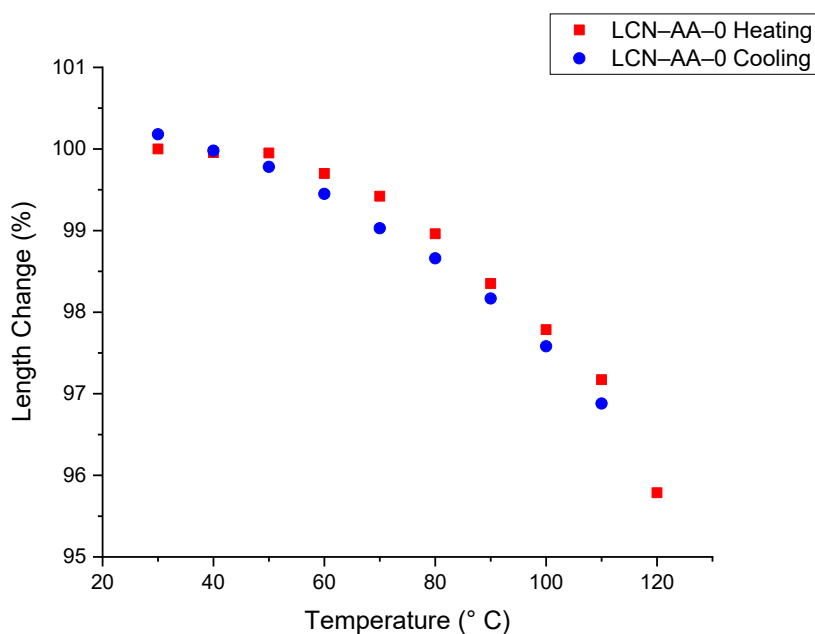
Table 7. Order parameter values for LCN films.

LCN Film	Order Parameter
LCN-AA-0	0.578
LCN-AA-1	0.592
LCN-AA-2	0.445
LCN-AA-3	0.104

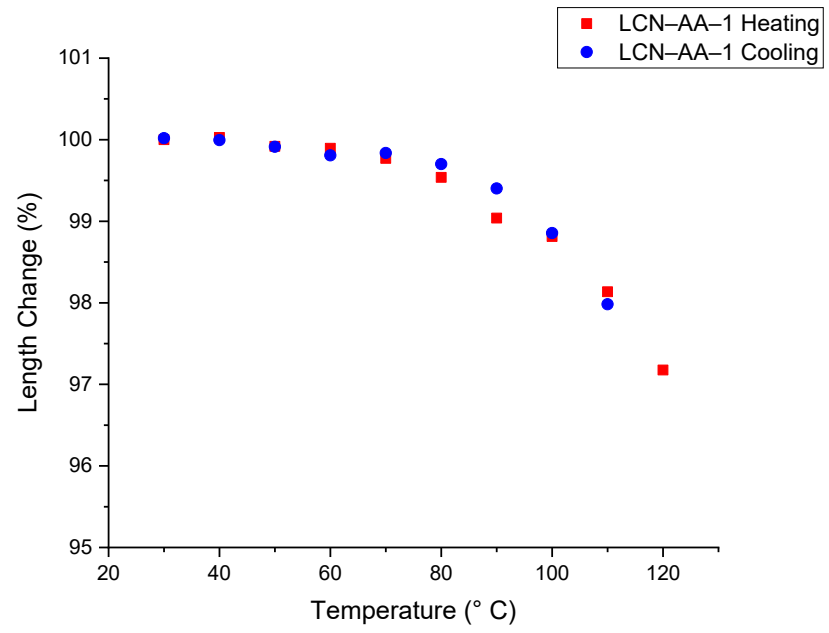
4.4.3 Thermal Actuation

Thermal actuation for the LCN films was tested using POM with the attachable heating/cooling stage. In typical LCN samples, first a plateau occurs, then a rapid decrease in length, then another plateau. The last plateau for the control sample was not observed until a temperature of 350° C was reached (Appendix A). As a result, it was initially decided to heat the samples from 30° C to 350° C, then cool back to 30° C. However, using these parameters on LCN-AA-1 resulted in the sample losing its ability to recover its original length when it was cooled down (Appendix B). Therefore, it was decided to proceed with lower final temperatures such as 120° C (section 3.4.3). Figure 13 shows the plots of the percentage of length change against the temperature for the four LCN samples. Upon reaching 120° C, the maximum length change for LCN films were as follows: LCN-AA-0 being the highest at 4.21%, LCN-AA-1 at 2.82%, LCN-AA-2 at 4.02%, and

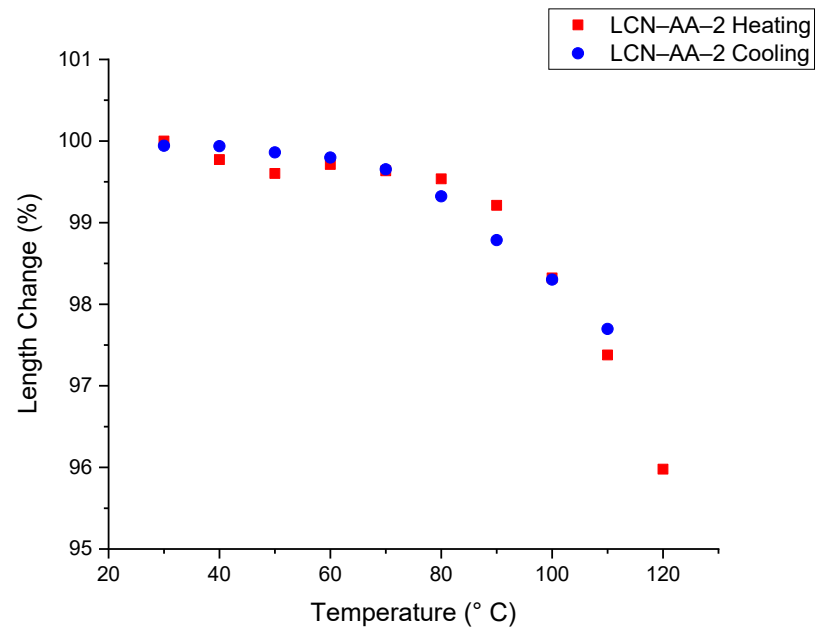
LCN-AA-3 being the lowest at a length change of 2.06%. The difference in the values was not significant, suggesting that the acrylic acid content ratio does not affect the contraction capacity of the LCN samples in 30-120° C temperature range. Moreover, all the LCN films were able to recover their original length when cooled down to 30° C, suggesting that the acrylic acid content ratio also does not affect the recovery capability of the LCN samples in 30-120° C temperature range. It is worth noting that in some plots, the final data point at cooling is higher than the initial data point at heating, which could imply an increase in the original length. However, the LCN samples might have been not fully relaxed on the surface of the coverslip at the beginning of the measurement, causing a slight reduction in the measurement of the original length of the sample.



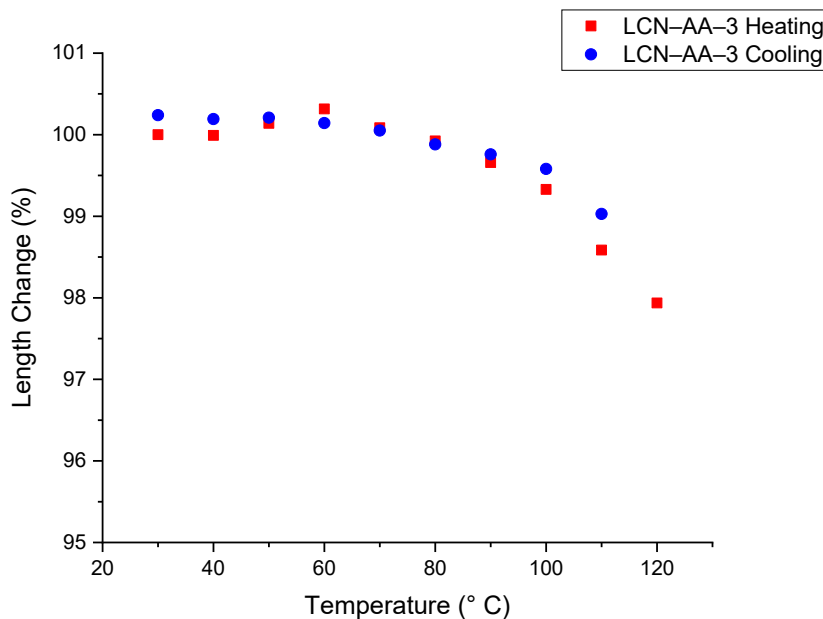
a) LCN-AA-0



b) LCN-AA-1



c) LCN-AA-2

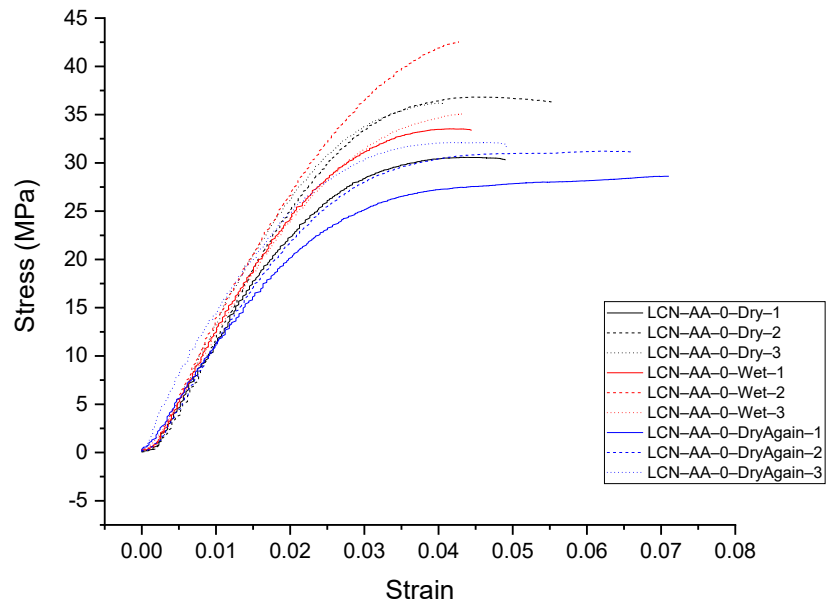


b) LCN-AA-3

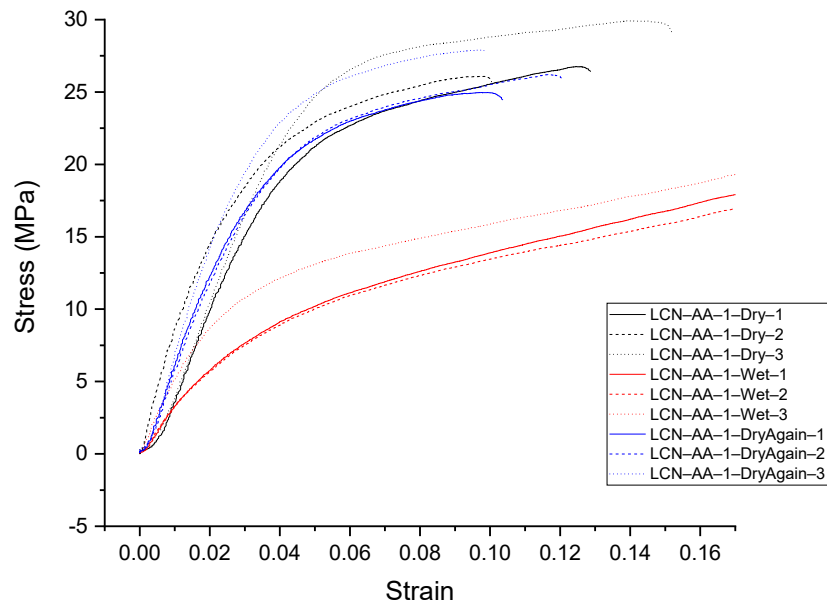
Figure 13. Plots of the length change percentage against the temperature for LCN films

4.4.4 Mechanical Properties and Adaptability

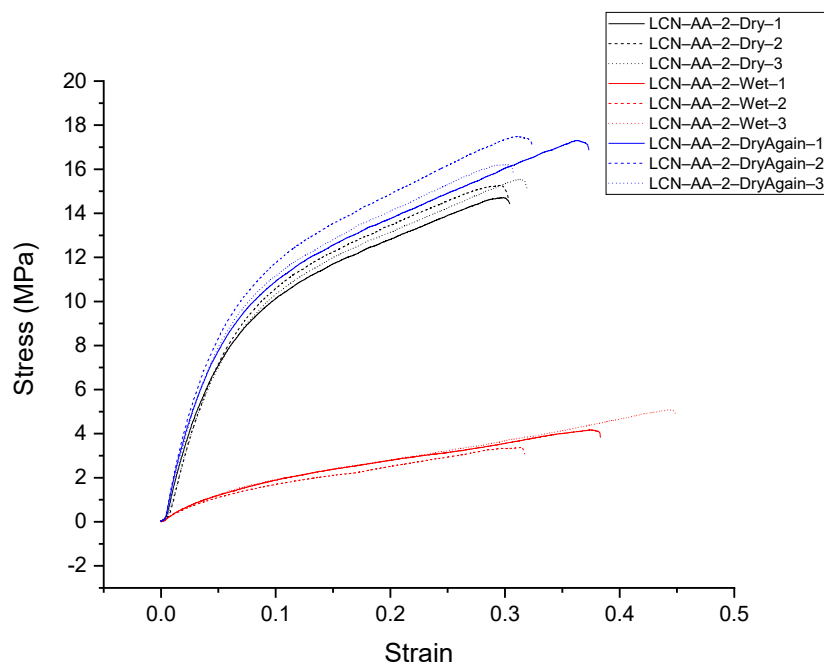
LCN-AA-0, LCN-AA-1, and LCN-AA-2 planar samples were tested using the tensile testing device. LCN-AA-3 planar samples were not tested due to difficulties in handling the stripes as they were not easily removed from the film. Stress-strain curves were plotted for the LCN samples in Figure 14. LCN-AA-0 did not show any significant changes from one condition to another (Figure 14.a). On the other hand, LCN-AA-1 and LCN-AA-2 plots showed significant changes between the three conditions (Figure 14.b and Figure 14.c). These observations suggest that LCN films containing acrylic acid, experienced a reversible change in their mechanical properties when changing from one condition to another.



a) LCN-AA-0



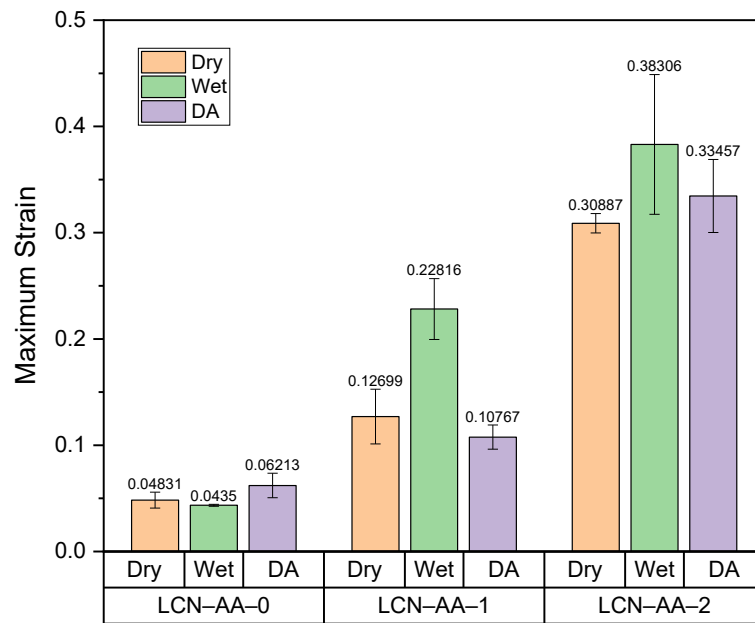
b) LCN-AA-1



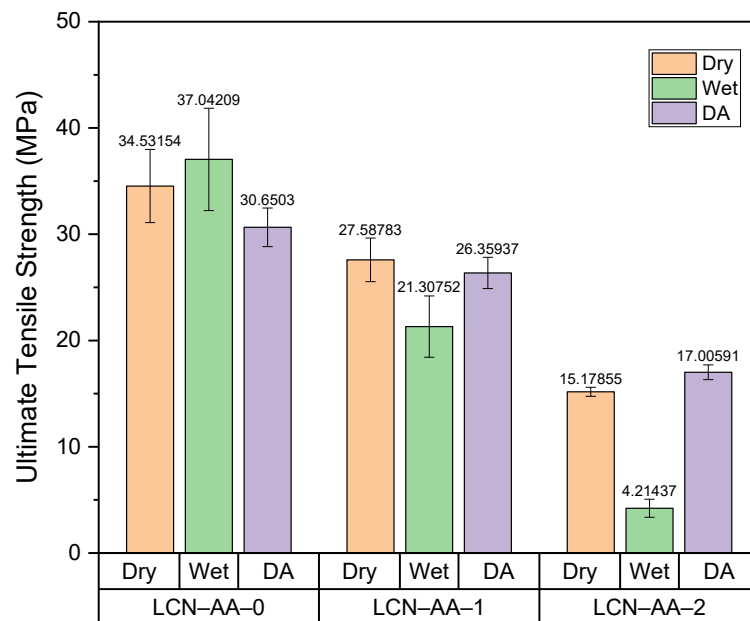
c) LCN-AA-2

Figure 14. Stress-strain curves for LCN films in different conditions

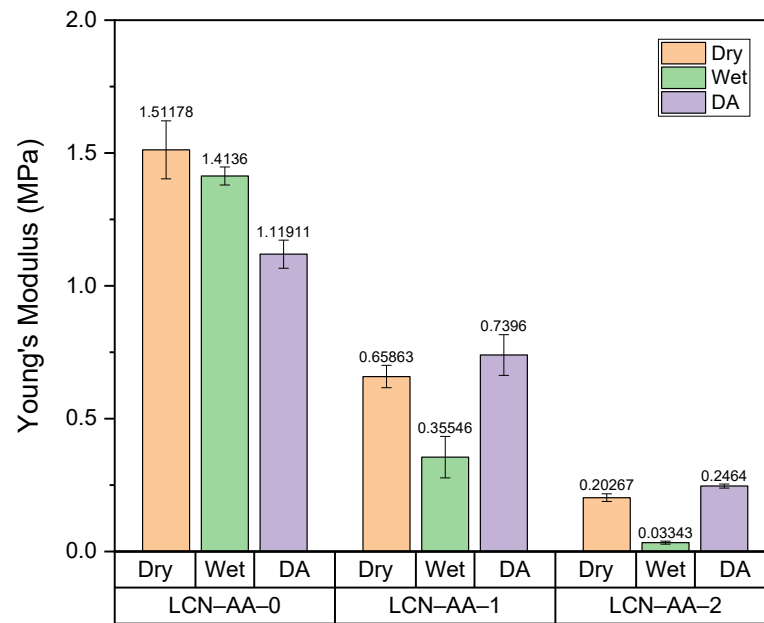
Average values of maximum strain before fracture point, UTS, and Young's modulus for the three conditions were plotted against the LCN film type in Figure 15. ϵ_{\max} , σ_{\max} and E were observed to differ in value from one LCN type to another, and from one condition to another for the same LCN type. Across all the LCN films in general, as the acrylic acid molar ratio increased, ϵ_{\max} increased, and σ_{\max} and E decreased. This suggests that adding acrylic acid into LC mixtures results in higher elasticity and lower tensile strength in their respective LCN films regardless of the condition surrounding the film. In LCN-AA-1 and LCN-AA-2, ϵ_{\max} experienced an increase in value from the dry condition to the wet condition, then decrease from the wet condition to the dry-again condition (Figure 15.a). The opposite effect was observed for σ_{\max} and E, where they experienced a decrease in value first then an increase (Figure 15.b and Figure 15.c). This suggests that the LCN samples experienced a reduction in their tensile strength and an increase in their elasticity when exposed to water and that reduction was reversed when the samples were dried up.



a) Changes in the maximum strain before fracture point



b) Changes in the ultimate tensile strength



c) Changes in Young's modulus

Figure 15. *Changes in LCN tensile properties in dry, wet and dry-again conditions.*

Percentage values of the relative change in Young's modulus in wet and dry-again conditions compared to dry condition were plotted in Figure 16. It showed that as M_{AA} decreases, the change percentage between the dry and wet conditions increases. These results support the claim that incorporating acrylic acid into LCN films offers mechanical adaptability feature for the LCN films, and as its amount increases, the changes in the mechanical properties from one condition to another increases.

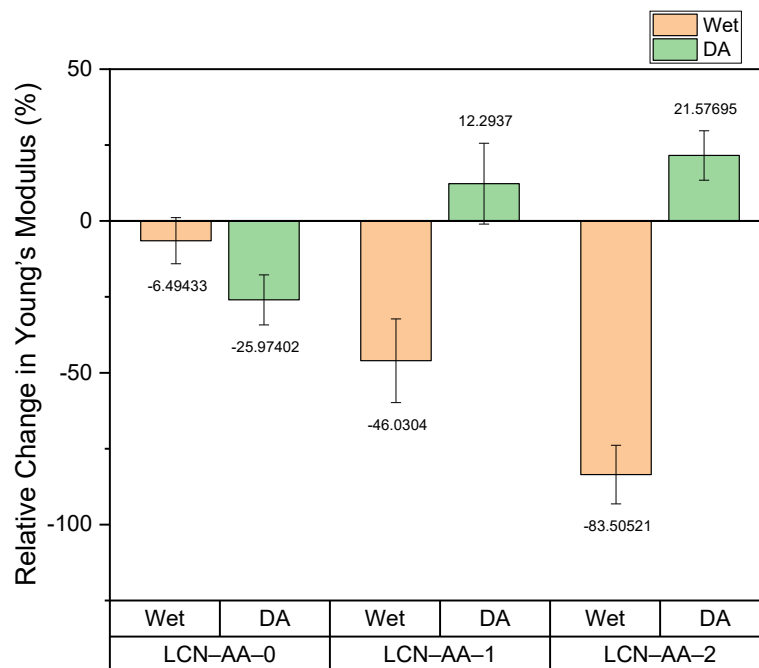


Figure 16. *Relative change of Young's modulus in wet and dry-again conditions compared to dry condition.*

4.4.5 Photothermal Actuation

LCN-AA-0, LCN-AA-1, and LCN-AA-2 splay samples were tested using a bending-tracking test. Figure 17 shows a splay sample before irradiation with light and after. Similar to section 4.4.4, LCN-AA-3 splay samples were not tested because they could not be easily removed from the film. Normalized bending angles were plotted against the light intensity for all the splay LCN samples in the three conditions as shown in Figure 18. In LCN-AA-1, the wet condition was conducted twice and were named "wet1" and "wet2".

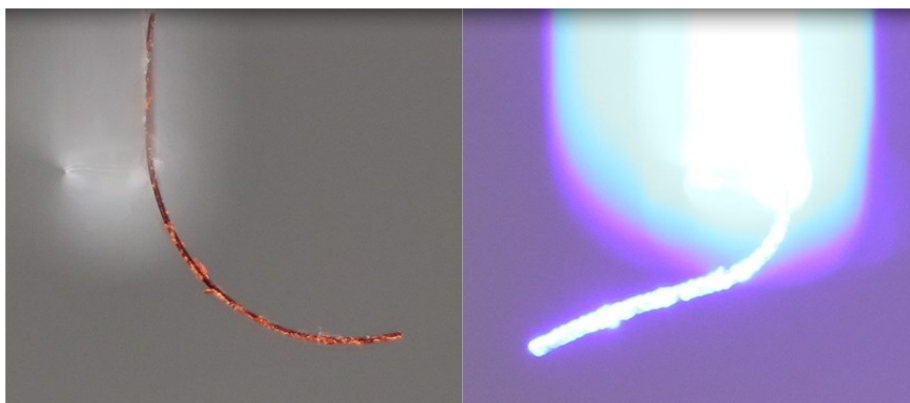
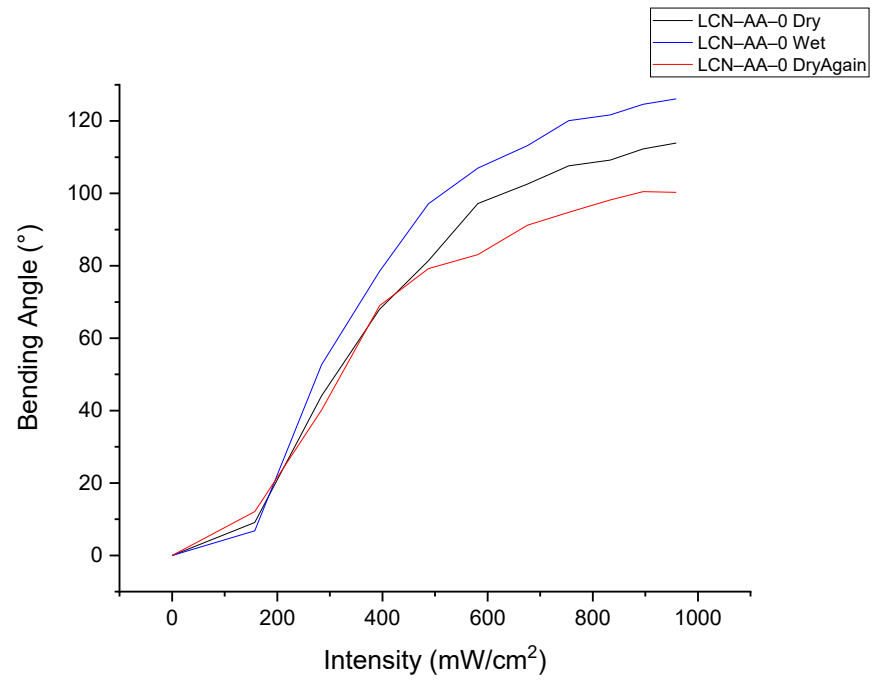
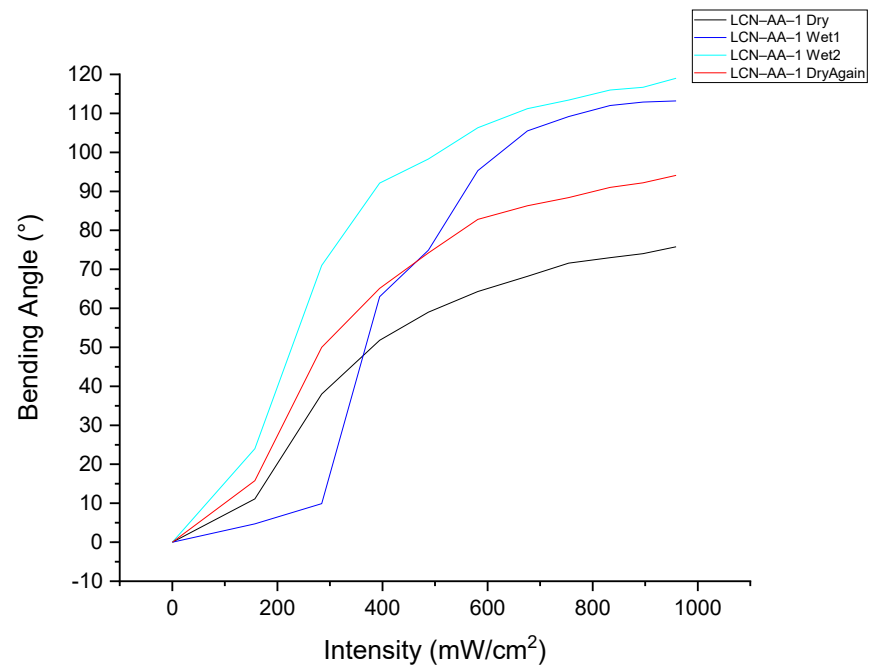


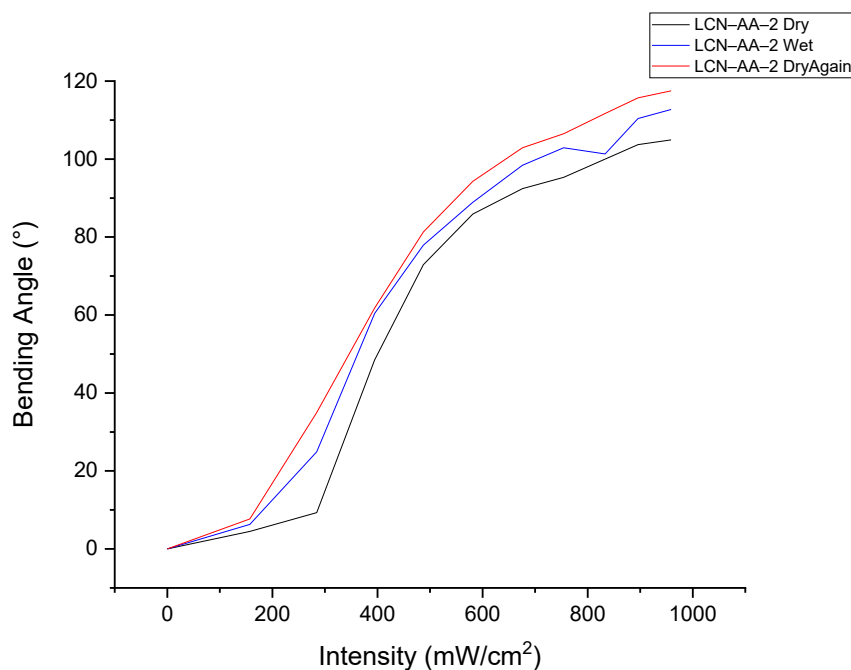
Figure 17. Bending of splay LCN samples; before irradiation (left) and after irradiation (right).



a) LCN-AA-0



b) LCN-AA-1



c) LCN-AA-2

Figure 18. Changes in normalized bending angle values for LCN samples against light intensity in different conditions.

In LCN-AA-0 and LCN-AA-2 samples, no significant changes were observed between the three conditions (Figure 18.a and Figure 18.c), however, the maximum bending angle (at maximum light intensity) was slightly different. On the other hand, LCN-AA-1 samples showed significant changes between the conditions (Figure 18.b). The pattern of the angles as well as the maximum bending angles were different. The pattern was also observed to change for the same condition when conducted multiple times (wet1 and wet2). Figure 19 highlights the changes in the maximum bending angle for splay LCN samples from one condition to another. LCN-AA-1 was observed to be the only film with the most significant change from the dry condition to the wet condition. Moreover, LCN-AA-1 managed to almost recover the original maximum bending angle in the dry-again condition.

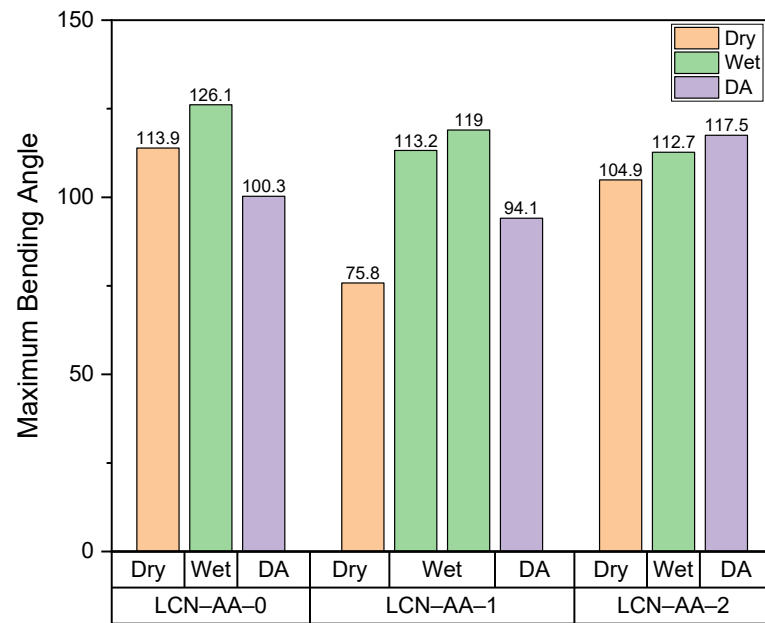


Figure 19. Changes in maximum bending angle values for LCN samples in different conditions. In LCN-AA-1, the two columns for the wet condition corresponds to wet1 and wet2.

5. CONCLUSIONS

Soft actuators have become an essential pivot in the soft robotics field, therefore, huge interest have been targeted towards enhancing soft actuators. One of the enhancements to be considered is the mechanical adaptability of such actuators. Incorporating a secondary network made of poly-acrylic acid into an LC network can produce a mechanical adaptability effect. In this thesis, mechanical adaptable light-responsive LCN films were successfully prepared from LC mixtures.

After preparing several LC mixtures with varied molar ratios of monomer to acrylic acid (M_{AA}), T_{NI} was identified for some of the LC mixtures and LCN films were polymerized from these LC mixtures. The prepared films were then characterized using few tests to assess structural and mechanical parameters. LCN films with M_{AA} of 1:1 (LCN-AA-1) and LCN films with M_{AA} of 1:2 (LCN-AA-2) showed the best performance in terms of the alignment quality, and the mechanical properties and adaptability. LCN-AA-1 films were superior in terms of the alignment and mechanical strength, while LCN-AA-2 films were superior in terms of the capacity of the mechanical adaptability.

A possible future work to this thesis is to test the LCNs in humid conditions and determine the relation between the humidity and the change in the mechanical properties of the LCNs. Moreover, ways to test LCNs underwater should be considered to assess the true behavior of such films in aquatic environments. Furthermore, compounds other than acrylic acid that can produce the same mechanical adaptability effect or better as well as other techniques of incorporation such as doping can be investigated and tested. Finally, designing and testing a soft robot made of mechanical adaptable light-responsive LCNs-based actuators is a promising step to be considered in the future.

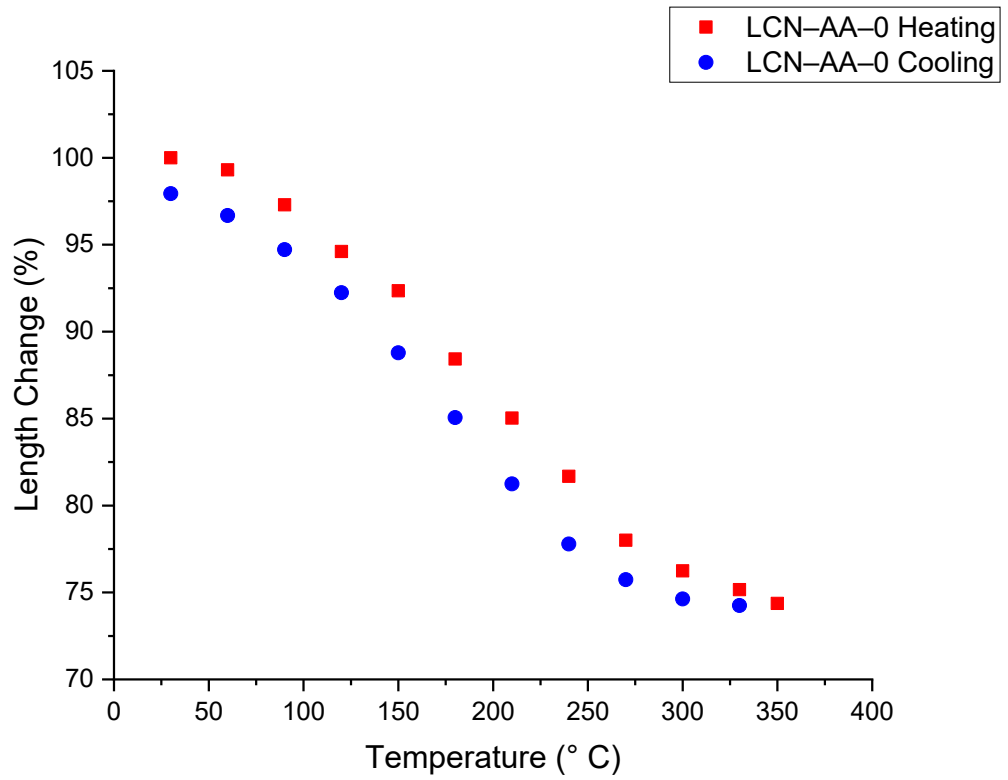
REFERENCES

- [1] J. Liu, Y. Gao, H. Wang, R. Poling-Skutvik, C.O. Osuji, S. Yang, Shaping and Locomotion of Soft Robots Using Filament Actuators Made from Liquid Crystal Elastomer–Carbon Nanotube Composites, *Adv. Intell. Syst.* 2 (2020) 1900163. <https://doi.org/10.1002/aisy.201900163>.
- [2] M. Pilz da Cunha, M.G. Debije, A.P.H.J. Schenning, Bioinspired light-driven soft robots based on liquid crystal polymers, *Chem. Soc. Rev.* 49 (2020) 6568–6578. <https://doi.org/10.1039/D0CS00363H>.
- [3] N. El-Atab, R.B. Mishra, F. Al-Modaf, L. Joharji, A.A. Alsharif, H. Alamoudi, M. Diaz, N. Qaiser, M.M. Hussain, Soft Actuators for Soft Robotic Applications: A Review, *Adv. Intell. Syst.* 2 (2020) 2000128. <https://doi.org/10.1002/aisy.202000128>.
- [4] Y. Dong, J. Wang, X. Guo, S. Yang, M.O. Ozen, P. Chen, X. Liu, W. Du, F. Xiao, U. Demirci, B.-F. Liu, Multi-stimuli-responsive programmable biomimetic actuator, *Nat. Commun.* 10 (2019) 4087. <https://doi.org/10.1038/s41467-019-12044-5>.
- [5] A. Gruzdenko, I. Dierking, Liquid crystal-based actuators, *Front. Soft Matter.* 2 (2022). <https://doi.org/10.3389/frsfm.2022.1052037>.
- [6] S.W. Ula, N.A. Traugutt, R.H. Volpe, R.R. Patel, K. Yu, C.M. Yakacki, Liquid crystal elastomers: an introduction and review of emerging technologies, *Liq. Cryst. Rev.* 6 (2018) 78–107. <https://doi.org/10.1080/21680396.2018.1530155>.
- [7] K.M. Herbert, H.E. Fowler, J.M. McCracken, K.R. Schlafmann, J.A. Koch, T.J. White, Synthesis and alignment of liquid crystalline elastomers, *Nat. Rev. Mater.* 7 (2021) 23–38. <https://doi.org/10.1038/s41578-021-00359-z>.
- [8] M.O. Astam, Y. Zhan, T.K. Slot, D. Liu, Active Surfaces Formed in Liquid Crystal Polymer Networks, *ACS Appl. Mater. Interfaces.* 14 (2022) 22697–22705. <https://doi.org/10.1021/acsami.1c21024>.
- [9] Y.-Y. Xiao, Z.-C. Jiang, Y. Zhao, Liquid Crystal Polymer-Based Soft Robots, *Adv. Intell. Syst.* 2 (2020) 2000148. <https://doi.org/10.1002/aisy.202000148>.
- [10] J. Calbo, C.E. Weston, A.J.P. White, H.S. Rzepa, J. Contreras-García, M.J. Fuchter, Tuning Azoheteroarene Photoswitch Performance through Heteroaryl Design, *J. Am. Chem. Soc.* 139 (2017) 1261–1274. <https://doi.org/10.1021/jacs.6b11626>.

- [11] A. Goulet-Hanssens, F. Eisenreich, S. Hecht, Enlightening Materials with Photoswitches, *Adv. Mater.* 32 (2020) 1905966. <https://doi.org/10.1002/adma.201905966>.
- [12] C. Toro, A. Thibert, L. De Boni, A.E. Masunov, F.E. Hernández, Fluorescence Emission of Disperse Red 1 in Solution at Room Temperature, *J. Phys. Chem. B.* 112 (2008) 929–937. <https://doi.org/10.1021/jp076026v>.
- [13] H. Shahsavan, A. Aghakhani, H. Zeng, Y. Guo, Z.S. Davidson, A. Priimagi, M. Sitti, Bioinspired underwater locomotion of light-driven liquid crystal gels, *Proc. Natl. Acad. Sci.* 117 (2020) 5125–5133. <https://doi.org/10.1073/pnas.1917952117>.
- [14] B. Li, L. Xu, Q. Wu, T. Chen, P. Sun, Q. Jin, D. Ding, X. Wang, G. Xue, A.-C. Shi, Various Types of Hydrogen Bonds, Their Temperature Dependence and Water–Polymer Interaction in Hydrated Poly(Acrylic Acid) as Revealed by ¹H Solid-State NMR Spectroscopy, *Macromolecules.* 40 (2007) 5776–5786. <https://doi.org/10.1021/ma070485c>.
- [15] D. Liu, D.J. Broer, Liquid Crystal Polymer Networks: Preparation, Properties, and Applications of Films with Patterned Molecular Alignment, *Langmuir.* 30 (2014) 13499–13509. <https://doi.org/10.1021/la500454d>.
- [16] H. Marsh, Carbon Mesophase, in: *Encycl. Mater. Sci. Technol.*, Elsevier, 2001: pp. 926–931. <https://doi.org/10.1016/B0-08-043152-6/00177-7>.
- [17] S.J.D. Lugger, S.J.A. Houben, Y. Foelen, M.G. Debije, A.P.H.J. Schenning, D.J. Mulder, Hydrogen-Bonded Supramolecular Liquid Crystal Polymers: Smart Materials with Stimuli-Responsive, Self-Healing, and Recyclable Properties, *Chem. Rev.* 122 (2022) 4946–4975. <https://doi.org/10.1021/acs.chemrev.1c00330>.
- [18] M.-M. Russev, S. Hecht, Photoswitches: From Molecules to Materials, *Adv. Mater.* 22 (2010) 3348–3360. <https://doi.org/10.1002/adma.200904102>.
- [19] M. Lahikainen, H. Zeng, A. Priimagi, Reconfigurable photoactuator through synergistic use of photochemical and photothermal effects, *Nat. Commun.* 9 (2018) 4148. <https://doi.org/10.1038/s41467-018-06647-7>.
- [20] I. Aprahamian, The Future of Molecular Machines, *ACS Cent. Sci.* 6 (2020) 347–358. <https://doi.org/10.1021/acscentsci.0c00064>.
- [21] J. Lall, H. Zappe, MEMS-compatible structuring of liquid crystal network actuators using maskless photolithography, *Smart Mater. Struct.* 31 (2022) 115014. <https://doi.org/10.1088/1361-665X/ac95e5>.

- [22] M. Todica, C. V. Pop, L. Udrescu, T. Stefan, Spectroscopy of a Gamma Irradiated Poly(Acrylic Acid)-Clotrimazole System, *Chinese Phys. Lett.* 28 (2011) 128201. <https://doi.org/10.1088/0256-307X/28/12/128201>.

APPENDIX A: THERMAL ACTUATION TEST FOR LCN-AA-0 AT HIGH TEMPERATURES



APPENDIX B: THERMAL ACTUATION TEST FOR LCN-AA-1 AT HIGH TEMPERATURES

